Anomalous scaling in homogeneous isotropic turbulence

2001 J. Phys. A: Math. Gen. 34 4389

(http://iopscience.iop.org/0305-4470/34/21/302)

INSTITUTE OF PHYSICS PUBLISHING JOURNAL OF PHYSICS A: MATHEMATICAL AND GENERAL

J. Phys. A: Math. Gen. **34** (2001) 4389–4435 www.iop.org/Journals/ja PII: S0305-4470(01)11206-0

Anomalous scaling in homogeneous isotropic turbulence

M J Giles

School of Engineering, University of Northumbria, Ellison Place, Newcastle upon Tyne. NE1 8ST, UK

Received 19 January 2000, in final form 1 February 2001

Abstract

The anomalous scaling exponents ζ_n of the longitudinal structure functions S_n for homogeneous isotropic turbulence are derived from the Navier–Stokes equations by using field theoretic methods to develop a low-energy approximation in which the Kolmogorov theory is shown to act effectively as a mean field theory. The corrections to the Kolmogorov exponents are expressed in terms of the anomalous dimensions of the composite operators which occur in the definition of S_n. These are calculated from the anomalous scaling of the appropriate class of nonlinear Green function, using an uv fixed point of the renormalization group, which thereby establishes the connection with the dynamics of the turbulence. The main result is an algebraic expression for ζ_n, which contains no adjustable constants. It is valid at orders n below g_*^{-1}, where g_* is the fixed point coupling constant. This expression is used to calculate ζ_n for orders in the range $n = 2$–10, and the results are shown to be in good agreement with experimental data, key examples being $\zeta_2 = 0.7$, $\zeta_3 = 1$ and $\zeta_6 = 1.8$.

PACS numbers: 0550, 4727

1. Introduction

The study of homogeneous isotropic turbulence has as its aim the derivation of the statistical features of small-scale velocity fluctuations at high Reynolds numbers, based on the assumption that they exhibit universal characteristics independent of the form of the large-scale flow structures [1–3]. A key quantity of interest is the longitudinal velocity increment, $v_+ - v_-$, where $v_\pm = v_1(x \pm r/2, y, z, t)$, the velocity component v_1 and the separation distance r both being in the same direction, here the x-axis. An empirical fact is that its nth order moment, the longitudinal structure function $S_n(r)$, defined by

$$S_n(r) = \left\langle (v_+ - v_-)^n \right\rangle \tag{1}$$

exhibits multiscaling. That is, the exponent ζ_n, defined by the scaling relation

$$S_n(r) \sim r^{\zeta_n} \tag{2}$$

0305-4470/01/214389+47$30.00

is a nonlinear function of the order n. This behaviour is not explained by the classical turbulence theory of Kolmogorov [4] which yields a linear dependence

$$\zeta_n^{\mathrm{Kol}} = \frac{n}{3}. \tag{3}$$

Moreover, the amount by which ζ_n differs from ζ_n^{Kol}, called the anomaly, has defied attempts at quantitative explanation [1–3, 5, 6]. The obstacle to progress with the theory is the strong nonlinearity of the governing Navier–Stokes (NS) equations. In this paper, our aim is to show how modern statistical field theory can be used to overcome this difficulty and provide theoretical predictions for ζ_n, which agree well with turbulent flow data.

The idea that statistical field theory can be brought to bear on the problem of turbulence is not itself new. Indeed, interest in describing turbulence in terms of the underlying functional probability distribution of the velocity field, together with its corresponding generating functional W, has a long history [5,6]. But such work has suffered from the weakness of relying on conventional perturbation theory to effect closure of the statistical hierarchy, whereas it is widely believed that a non-perturbative treatment is necessary, because the NS equations lack a small parameter. Consequently, progress with this approach has been disappointing.

The question is whether we can find a middle course, which avoids the limitations of conventional perturbation theory, while not demanding an intractable non-perturbative approach. Here we explore the possibility of formulating a more efficient perturbation theory by developing a zero-order solution which already accounts for the dominant nonlinear interactions, in an attempt, as it were, to deplete the effect of the nonlinearity. We shall do this by adopting a more general quadratic form in W in place of the viscous form which arises naturally. The modified quadratic form is determined self-consistently from the NS nonlinearity using the linear response function and the energy equation. In the inertial range, it leads directly to the Kolmogorov distribution, after allowing for the kinematic effect of the sweeping of the smaller scales by the larger ones. The difference between these quadratic forms then appears as a perturbation, which, as we shall see, is not critical, provided that the force spectrum function is non-zero only at small wavenumbers and yields a finite input power.

Having incorporated the dominant nonlinearities which are responsible for the turbulence energy cascade into the zero-order solution, what is then lacking is the effect of the fluctuating dissipation rate, which is the well known defect of the Kolmogorov theory [5]. In this approach, the perturbation theory is then, in effect, only required to accommodate the residual coupling associated with these fluctuations, which are directly responsible for the anomalies. The fact that the anomalies are small, and associated with a weak residual coupling, provides good reason to expect that a small expansion parameter might emerge, thereby rendering the problem accessible to perturbation theory, essentially by means of a standard loop-expansion of the generating functional.

Although the use of the modified quadratic form as an initial approximation would appear to be an attractive option, providing a sound physical basis for the approximate evaluation of the generating functional, it poses severe technical problems, the most significant being the occurrence of divergences at higher orders in perturbation theory, due to the incomplete representation of the large-scale flow. These divergences are of two types: power divergences (including power $\times$ logarithmic), which are associated with the sweeping, and pure logarithmic divergences, which describe the cascade process. On the other hand, statistical field theory [7], provides the mathematical techniques needed to compensate for such divergences, in the form of the well known processes of resummation and renormalization. In particular, renormalization [8] provides a procedure whereby the scale invariance in (2) can be recovered from a divergent theory, yielding the exponents in terms of the anomalous dimensions of the composite operators appearing in (1), which we can calculate from the appropriate nonlinear

Green functions. The modified quadratic form itself follows uniquely from the requirement for the absence of non-renormalizable terms, after renormalizing the basic parameters of W and allowing for sweeping.

Fortunately, sweeping effects do not pose an insuperable obstacle, notwithstanding that the initial formulation is Eulerian. Indeed, we show that the power divergences associated with sweeping can be removed by introducing a single sweeping interaction term, which can be derived from the generating functional itself by transforming to a frame moving with the local velocity of the large scale eddies, using a random Galilean transformation of the velocity field, having an rms convection speed which is calculated from the NS nonlinearity. The application of this transformation does not, of course, affect the values of $S_n(r)$ and, thus, enables the straining interactions which determine the spectrum to be separated from the background of sweeping convection, yielding, in effect, quasi-Lagrangian forms. In this way, as we shall show below, it proves possible to demonstrate multiscaling and calculate the anomalies of the structure functions accurately.

2. Theoretical foundations

Our starting point is the NS equations, describing flow in an incompressible fluid of unit density, velocity $\boldsymbol{v}$, kinematic viscosity $\bar{\nu}$ and pressure p, and driven by a random solenoidal stirring force $\boldsymbol{f}$, which are

$$\frac{\partial \boldsymbol{v}}{\partial t} + \boldsymbol{v} \cdot \boldsymbol{\nabla} \boldsymbol{v} = -\nabla p + \bar{\nu} \nabla^2 \boldsymbol{v} + \boldsymbol{f} \tag{4}$$

and

$$\operatorname{div} \boldsymbol{v} = 0. \tag{5}$$

Suppose that

$$\boldsymbol{v}(\hat{x}) = \boldsymbol{V}(\hat{x}|\boldsymbol{f}) \tag{6}$$

is the solution of (4) at the space–time point $\hat{x} = (\boldsymbol{x}, t)$, corresponding to a force $\boldsymbol{f}(\hat{x})$, which has a Gaussian probability distribution $\mathcal{P}(\boldsymbol{f})$. Then the generating functional W for the correlation functions of the velocity field can be written as the functional integral

$$W = \int \exp(S) \mathcal{P}(\boldsymbol{f}) \, \mathcal{D}\boldsymbol{f} \tag{7}$$

where the source term is given by

$$S(\boldsymbol{J}) = \int \boldsymbol{J}(\hat{x}) \cdot \boldsymbol{V}(\hat{x}|\boldsymbol{f}) \, \mathrm{d}\hat{x} \tag{8}$$

and the correlators follow by functional differentiation with respect to the source field $\boldsymbol{J}(\hat{x})$. Given that we cannot obtain an explicit expression for the solution (6), the crux of the problem is how to approximate (7) with the accuracy required to calculate the ζ_n. In our approach, as indicated above, we prove that the Kolmogorov theory can be used effectively as a mean field theory in a saddle-point evaluation of (7), and that this leads to an expansion which has a genuinely small coupling constant.

Within the context of a field theoretic interpretation of (7), each term of the binomial expansion of (1) must be regarded as an operator product of the usual Wilson type, (see e.g. [7, 8]). Correspondingly, the powers of $v_\pm$ must be treated as composite operators, which, in accordance with standard procedures [7], must be generated from W by independent sources. However, in defining a suitable set of longitudinal composite operators, we must take account of the fact that, whereas the velocity difference $v_+ - v_-$, and, hence, $S_n(r)$, is dominated

by motions of scale r, and, thus, can be expected to display universal features, when r is in the inertial range, the same is not true of the velocities $v_\pm$ themselves, because, relative to the laboratory frame, they include contributions from the large-scale eddies. These must be eliminated, which can be accomplished by referring the flow to a frame moving with the local velocity $\boldsymbol{U}$ of the large-scale eddies, as discussed fully in section 7. Here, our aim is to limit the composite operators that need to be allowed for to those which appear explicitly in the definition of $S_n(r)$, as given in (1). Indeed, rewriting (1) in the form

$$S_n(r) = \left\langle \{(v_+ - U_1) - (v_- - U_1)\}^n \right\rangle$$

leads one to define a set of longitudinal Galilean invariant composite operators $O_s(\hat{x})$, for $s = 2, 3, 4, \ldots$, relative to the laboratory frame, by

$$O_s(\hat{x}|\boldsymbol{f}) = [V_1(\hat{x}|\boldsymbol{f}) - U_1]^s/s! \tag{9}$$

which we generate from W by adding to the source term (8), the additional term

$$-\sum_s \int t_s(\hat{x})\, O_s(\hat{x}|\boldsymbol{f})\, \mathrm{d}\hat{x}. \tag{10}$$

We also need to include in the definition of W a means of establishing the vital link between the time-independent definition of $S_n(r)$ and the dynamics of the turbulence. This requires the introduction of a dynamic response operator, which we define to be the functional differentiation operator

$$\mathcal{F}_\alpha(\hat{x}) = \frac{\delta}{\mathrm{i}\delta f_\alpha(\hat{x})}. \tag{11}$$

Its inclusion in the definition of W adds a final source term to S, given by

$$\int J_\alpha(\hat{x})\mathcal{F}_\alpha(\hat{x})\, \mathrm{d}\hat{x} \tag{12}$$

where summation over repeated vector indices is implied here and below.

The terms (8), (10) and (12) together constitute the full source term for (7) which becomes, therefore,

$$S(\boldsymbol{J}, \tilde{\boldsymbol{J}}, t_s) = \int \left\{ J_\alpha(\hat{x}) V_\alpha(\hat{x}|\boldsymbol{f}) + \tilde{J}_\alpha(\hat{x})\mathcal{F}_\alpha(\hat{x}) - \sum_s t_s(\hat{x})\, O_s(\hat{x}|\boldsymbol{f}) \right\} \mathrm{d}\hat{x} \tag{13}$$

and this completes the definition of W. Thus, (7) and (13) provide the foundation of our approach to the calculation of ζ_n. However, before we can proceed with this calculation, we must cast W into a conventional field theory form, and introduce the modified quadratic form.

A straightforward method of transforming (7) into a conventional field theory form is to replace $\mathcal{P}(\boldsymbol{f})$ by its functional Fourier transform and then integrate over $\boldsymbol{f}$. This is the stage at which we make explicit use of the NS equations. Essentially, to effect the transformation, we change our perspective by replacing the velocity field $\boldsymbol{V}(\boldsymbol{f})$ generated by the force $\boldsymbol{f}$, by the force $\boldsymbol{F}(\boldsymbol{v})$ needed to excite a particular realization $\boldsymbol{v}$ of the flow field. The operator (11) is then replaced by an equivalent conjugate vector field $\tilde{\boldsymbol{v}}$.

To carry out this transformation, we work in the Fourier domain setting

$$\boldsymbol{v}(\hat{x}) = \int \exp(\mathrm{i}\hat{k}\cdot\hat{x})\, \boldsymbol{v}(\hat{k})\, \mathrm{D}\hat{k}$$

where $\hat{k}$ denotes $(\boldsymbol{k}, \omega)$, so that $\hat{k}\cdot\hat{x} = \omega t - \boldsymbol{k}\cdot\boldsymbol{x}$, while $\mathrm{D}\hat{k} = \mathrm{d}\omega\, \mathrm{d}\boldsymbol{k}/(2\pi)^4$. Then, from (4) and (5), we have

$$F_\alpha(\hat{k}, \boldsymbol{v}) = G_0(\hat{k})^{-1} v_\alpha(\hat{k}) - \frac{\mathrm{i}}{2}(2\pi)^4 P_{\alpha\beta\gamma}(\boldsymbol{k}) \int v_\beta(\hat{p}) v_\gamma(\hat{q}) \delta(\hat{p} + \hat{q} - \hat{k})\, \mathrm{D}\hat{p}\, \mathrm{D}\hat{q}. \tag{14}$$

The notation here is the following. $G_0(\hat{k})$ is the zero-order approximation to the response function $G(\hat{k})$ defined below in (70) and (71), namely

$$G_0(\hat{k}) = \frac{1}{\mathrm{i}\omega + \tau_v(k)^{-1}} \tag{15}$$

where

$$\tau_v(k)^{-1} = \bar{\nu}k^2.$$

$P_{\alpha\beta\gamma}(\boldsymbol{k})$ is the NS vertex defined by

$$P_{\alpha\beta\gamma}(\boldsymbol{k}) = k_\beta P_{\alpha\gamma}(\boldsymbol{k}) + k_\gamma P_{\alpha\beta}(\boldsymbol{k}) \tag{16}$$

where

$$P_{\alpha\beta}(\boldsymbol{k}) = \delta_{\alpha\beta} - k_\alpha k_\beta / k^2. \tag{17}$$

Next we write the Gaussian distribution of $\boldsymbol{f}$ in the form

$$\mathcal{P}(\boldsymbol{f}) = \mathcal{N} \exp\left\{-\tfrac{1}{2}\int f_\alpha(-\hat{k})h(k)^{-1}P_{\alpha\beta}(\boldsymbol{k})f_\beta(\hat{k})\,\mathrm{D}\hat{k}\right\} \tag{18}$$

for which the corresponding force covariance is

$$\left\langle f_\alpha(\hat{k})f_\beta(\hat{l})\right\rangle = (2\pi)^4\delta(\hat{k}+\hat{l})h(k)P_{\alpha\beta}(\boldsymbol{k})$$

where the force spectrum function $h(k)$ is an arbitrary function which is assumed to be peaked near the origin, so that the power input $\int h(k)\,\mathrm{d}\boldsymbol{k}$ is finite. Otherwise, we make no specific assumptions regarding the form of $h(k)$. We now change the functional integration over $\boldsymbol{f}$ in (7) to an integration over $\boldsymbol{v}$ by means of the transformation $\boldsymbol{v}(\hat{k}) = \boldsymbol{V}(\hat{k}|\boldsymbol{f})$, and substitute the representation

$$\mathcal{P}(\boldsymbol{f}) = \mathcal{N}\int \exp\left\{-\tfrac{1}{2}\int \tilde{v}_\alpha(-\hat{k})h(k)P_{\alpha\beta}(\boldsymbol{k})\tilde{v}_\beta(\hat{k})\,\mathrm{D}\hat{k} + \mathrm{i}\int \tilde{v}_\alpha(-\hat{k})f_\alpha(\hat{k})\,\mathrm{D}\hat{k}\right\}\mathcal{D}\tilde{\boldsymbol{v}}. \tag{19}$$

Since the Jacobian only contributes an unimportant constant, we get

$$W(\boldsymbol{J},\tilde{\boldsymbol{J}},t_\mathrm{s}) = \int \exp\big[-L(\boldsymbol{v},\tilde{\boldsymbol{v}}) + S(\boldsymbol{J},\tilde{\boldsymbol{J}},t_\mathrm{s})\big]\mathcal{D}\boldsymbol{v}\,\mathcal{D}\tilde{\boldsymbol{v}} \tag{20}$$

where

$$L(\boldsymbol{v},\tilde{\boldsymbol{v}}) = \tfrac{1}{2}\int \tilde{v}_\alpha(-\hat{k})h(k)P_{\alpha\beta}(\boldsymbol{k})\tilde{v}_\beta(\hat{k})\,\mathrm{D}\hat{k} - \mathrm{i}\int \tilde{v}_\alpha(-\hat{k})F_\alpha(\hat{k},\boldsymbol{v})\,\mathrm{D}\hat{k} \tag{21}$$

while the source term (13) becomes

$$S(\boldsymbol{J},\tilde{\boldsymbol{J}},t_\mathrm{s}) = \int\left\{J_\alpha(-\hat{k})v_\alpha(\hat{k}) + \tilde{J}_\alpha(-\hat{k})\tilde{v}_\alpha(\hat{k}) - \sum_\mathrm{s} t_\mathrm{s}(-\hat{k})O_\mathrm{s}(\hat{k})\right\}\mathrm{D}\hat{k} \tag{22}$$

where $O_\mathrm{s}(\hat{k})$ is the Fourier transform of

$$O_\mathrm{s}(\hat{x}) = \big[v_1(\hat{x}) - U_1\big]^s/s!. \tag{23}$$

The expression (20) casts W into the form of an MSR-type functional integral [9].

Now the quadratic form appearing in (21) does not provide a good initial approximation for inertial range scaling, because, of course, it merely describes the viscous decay of an externally driven random flow, with no account taken of the nonlinear interactions. It is thus essential in developing an expansion theorem for (20) to introduce a more appropriate quadratic form. Here, we can appeal to the general theory of quadratic forms in a Hilbert space which indicates that we can introduce at most two functions.These can be taken as an apparent force spectrum

$D_0(k)$ and an effective micro-timescale $\tau_0(k)$, which are related to the energy in wavemode $\boldsymbol{k}$, $Q(k)$, by

$$Q(k) = \tfrac{1}{2}\tau_0(k) D_0(k). \tag{24}$$

The modified quadratic form in $L(\boldsymbol{v}, \tilde{\boldsymbol{v}})$ is then obtained, firstly, by replacing $h(k)$ with $D_0(k)$ and, secondly, by replacing the viscous timescale $\tau_\nu(k)$ by the the effective timescale $\tau_0(k)$, so that the viscous propagator (15) in (14) is replaced by

$$G_0(\hat{k}) = \frac{1}{\mathrm{i}\omega + \tau_0(k)^{-1}}. \tag{25}$$

Thus, we now have in place of (21)

$$L(\boldsymbol{v}, \tilde{\boldsymbol{v}}) = \tfrac{1}{2}\int \tilde{v}_\alpha(-\hat{k}) D_0(k) P_{\alpha\beta}(\boldsymbol{k}) \tilde{v}_\beta(\hat{k})\, \mathrm{D}\hat{k} - \mathrm{i}\int \tilde{v}_\alpha(-\hat{k}) F_\alpha(\hat{k}, \boldsymbol{v})\, \mathrm{D}\hat{k} \tag{26}$$

in which $D_0(k)$ and $\tau_0(k)$ are, as yet, unknown functions to be determined later from a solvability condition associated with the energy equation and the linear response function. The idea that one should replace the viscous quadratic form by a modified form was suggested originally in [10], where it was used in conjunction with a variational principle based on an entropy functional, but recent work [11] has shown that this approach contains an arbitrary element. However, we shall not need to invoke any additional principle, because we shall be able to deduce the modified quadratic form in a self-consistent way from the 1-loop expansion, as we have already indicated.

The introduction of the modified quadratic form as a basis for an expansion theorem for (20) requires the inclusion of the difference terms as perturbations, which contributes an additional term to L given by

$$\begin{aligned}\Delta L_0 = \tfrac{1}{2}\int \tilde{v}_\alpha(-\hat{k})\{h(k) - D_0(k)\} P_{\alpha\beta}(\boldsymbol{k}) \tilde{v}_\beta(\hat{k})\, \mathrm{D}\hat{k} \\ - \mathrm{i}\int \tilde{v}_\alpha(-\hat{k})\{\tau_\nu(k)^{-1} - \tau_0(k)^{-1}\} v_\alpha(\hat{k})\, \mathrm{D}\hat{k}.\end{aligned} \tag{27}$$

These terms have the same form as the counterterms introduced below in (33) to accommodate the pure logarithmic divergences but their role, as we shall see, is not critical as regards calculating the inertial range exponents.

The derivation of the form of the functions $D_0(k)$ and $\tau_0(k)$ occurring in the modified quadratic form entails a detailed discussion of sweeping convection, the structure of the Feynman diagrams associated with the loop expansion of W and the establishment of the solvability condition for the absence from the linear response function of non-renormalizable terms. We shall defer detailed discussion of these topics until sections 7 and 8 and, meanwhile, proceed with the calculation of the anomalous exponents by anticipating their forms, which, in the inertial range, are

$$D_0(k) = D_0 k^{-3} \tag{28}$$

and

$$\tau_0(k)^{-1} = \nu_0 k^{2/3}. \tag{29}$$

Clearly, these forms imply that the zero-order solution behaves in the inertial range *as if* the fluid were stirred by a random force with a k^{-3} force correlation spectrum, to which it responds with a Lagrangian timescale $\propto k^{-2/3}$, even though the actual force spectrum $h(k)$ is an arbitrary function which is peaked near $k = 0$. Thus, they lead to the Kolmogorov distribution. We shall explain how this result follows from the generating functional in section 8. The advantage of

this approximation is that it achieves a prime requirement of any efficient perturbation theory, which is a zero-order approximation that already closely approximates the desired solution.

On the other hand, as we have indicated, the resulting perturbation theory yields divergences at higher orders. But we shall find that, provided the flow is referred to a frame moving with the local velocity $\boldsymbol{U}$ of the large-scale eddies, these divergences can be handled by standard renormalization procedures. Thus, all calculations will be referred to this moving frame. As we will show in section 7, the effect of this change of frame, is to introduce an additional sweeping interaction term into L given by

$$\Delta L_{\mathrm{s}} = \frac{3}{4}\frac{g\nu^3}{\tau(\kappa)}\int \boldsymbol{l}\cdot\boldsymbol{m}\,\tilde{\boldsymbol{v}}(\hat{m})\cdot\boldsymbol{v}(-\hat{m})\tilde{\boldsymbol{v}}(\hat{l})\cdot\boldsymbol{v}(-\hat{l})\,\mathrm{D}\hat{l}\,\mathrm{D}\hat{m} \tag{30}$$

which cancels the contributions to the probability associated with the sweeping convection generated by the NS vertex. In particular, it eliminates the power divergences which, as indicated above, arise from the kinematic effect of the sweeping of small scales by larger scales. So (30) provides a means of regularizing the theory apart from the pure logarithmic divergences, which we can sum by renormalization group methods to obtain ζ_n. The structure functions (1) are, of course, invariant under this change of frame, while (23) becomes

$$O_{\mathrm{s}}(\hat{x}) = v_1(\hat{x})^s/s! \tag{31}$$

so that

$$O_{\mathrm{s}}(\hat{k}) = v_1(\hat{k})^s/s!$$

where $v_1(\hat{k})^s$ denotes the Fourier transform of $v_1(\hat{x})^s$. For ease of notation, we do not distinguish between $\boldsymbol{v}$ and $\tilde{\boldsymbol{v}}$ before and after the Galilean transformation. As all calculations are to be carried out in the moving frame this should cause no confusion.

Thus, an important implication of using the modified quadratic form as an initial approximation for the calculation of ζ_n is that renormalization becomes a necessary preliminary. So we need to identify the counterterms which arise in W under renormalization and obtain the transformation rule which connects the bare and renormalized generating functionals. Renormalization is applied to the viscosity and force constants appearing in (28) and (29) in the usual way by introducing renormalization constants Z_ν and Z_D, which relate their bare values ν_0 and D_0 to their renormalized replacements ν and D by

$$\nu_0 = \nu Z_\nu \qquad \text{and} \qquad D_0 = DZ_D. \tag{32}$$

This generates counterterms in (21) for the elementary fields ($\boldsymbol{v}$ and $\tilde{\boldsymbol{v}}$) given by

$$\Delta L_{\mathrm{ef}} = -\Delta Z_\nu \mathrm{i}\int \tilde{v}_\alpha(-\hat{k})\tau(k)^{-1}v_\alpha(\hat{k})\mathrm{D}\hat{k} + \Delta Z_D\tfrac{1}{2}\int \tilde{v}_\alpha(-\hat{k})\,D(k)P_{\alpha\beta}(\boldsymbol{k})\tilde{v}_\alpha(\hat{k})\,\mathrm{D}\hat{k} \tag{33}$$

where we have defined renormalization constant increments by

$$\Delta Z_{\nu,D} = Z_{\nu,D} - 1.$$

The additional renormalization which must be applied to the composite operators (31) also takes the standard form

$$(O_{\mathrm{s}})_{\mathrm{B}} = Z_{\mathrm{s}}(O_{\mathrm{s}})_{\mathrm{R}}. \tag{34}$$

The corresponding counterterm is obtained by substituting (34) in (22) to get

$$\Delta L_{\mathrm{co}} = \sum_{\mathrm{s}} \Delta Z_{\mathrm{s}} \int t_{\mathrm{s}}(-\hat{k})\,O_{\mathrm{s}}(\hat{k})\,\mathrm{D}\hat{k}$$

where

$$\Delta Z_{\mathrm{s}} = Z_{\mathrm{s}} - 1.$$

We conclude this section by giving the transformation which relates the generating functional of the bare correlation functions W_{B} to its corresponding renormalized form W_{R}. To provide a convenient means of handling the dependence of the correlation and response functions on the dimensional parameters ν_0 and D_0, we rescale $\boldsymbol{V}$ and $\boldsymbol{f}$ by introducing bare fields defined by

$$\boldsymbol{V}(\hat{k}) = \left(\frac{D_0}{\nu_0^3}\right)^{\frac{1}{2}} \boldsymbol{V}_{\mathrm{B}}(\boldsymbol{k}, \omega_{\mathrm{B}})$$

and

$$\boldsymbol{f}(\hat{k}) = \left(\frac{D_0}{\nu_0}\right)^{\frac{1}{2}} \boldsymbol{f}_{\mathrm{B}}(\boldsymbol{k}, \omega_{\mathrm{B}})$$

with bare frequency

$$\omega_{\mathrm{B}} = \frac{\omega}{\nu_0}.$$

These bare fields preserve the form of the NS equations, apart from explicitly introducing the non-dimensional coupling constant, defined by

$$g_0 = \frac{D_0}{6\pi^2 \nu_0^3} \tag{35}$$

in which the appropriateness of the numerical factor will appear later from the loop-expansion of W.

Under the renormalization (32), the bare fields are replaced by renormalized fields, to which they are related by

$$\boldsymbol{V}_{\mathrm{B}}(\boldsymbol{k}, \omega_{\mathrm{B}}) = \left(\frac{Z_\nu^3}{Z_D}\right)^{\frac{1}{2}} \boldsymbol{V}_{\mathrm{R}}(\boldsymbol{k}, \omega_{\mathrm{R}})$$

and

$$\boldsymbol{f}_{\mathrm{B}}(\boldsymbol{k}, \omega_{\mathrm{B}}) = \left(\frac{Z_\nu}{Z_D}\right)^{\frac{1}{2}} \boldsymbol{f}_{\mathrm{R}}(\boldsymbol{k}, \omega_{\mathrm{R}})$$

where

$$\omega_{\mathrm{R}} = \frac{\omega}{\nu}.$$

These relations follow from two requirements. First, the form of the NS equations (14) must again be preserved, with the new constants ν and D resulting in a renormalized coupling constant

$$g = \frac{D}{6\pi^2 \nu^3}. \tag{36}$$

Second, we have to satisfy the crucial requirement that $\mathcal{P}(\boldsymbol{f})$, as given in (18), remains invariant under renormalization. Indeed, satisfaction of these conditions implies the desired relation between W_{B} and W_{R}, which from (20) and (22), is readily found to be

$$W_{\mathrm{R}}(\boldsymbol{J}, \tilde{\boldsymbol{J}}, t_{\mathrm{s}}) = W_{\mathrm{B}}\left(\frac{1}{Z_\nu}\left(\frac{Z_D}{Z_\nu}\right)^{1/2} \boldsymbol{J},\ \frac{1}{Z_\upsilon}\left(\frac{Z_\upsilon}{Z_D}\right)^{1/2} \tilde{\boldsymbol{J}},\ \frac{Z_{\mathrm{s}}}{Z_\nu^s}\left(\frac{Z_D}{Z_\nu}\right)^{s/2} t_{\mathrm{s}}\right). \tag{37}$$

The foregoing provides the basis of our calculation of ζ_n, which involves the following four stages, all of which are carried out relative to the moving frame. First, we use (37) and the binomial expansion of (1) to develop a short distance expansion for $S_n(r)$, by substituting an operator product expansion (OPE) [7,8] for each term, based on the operators (31) applying in

the moving frame. As shown in section 3, this yields the scaling of $S_n(r)$ in terms of uv fixed point values of standard RG functions. The second stage of the calculation is to demonstrate that the required uv fixed point of the RG actually exists, and then to deduce the corresponding fixed point coupling constant g_*. This is done in section 4 by considering the renormalization of the linear response function, using the renormalized functional in the form obtained from (25) and (26). The third stage is to calculate the specific fixed point RG parameters which give the anomalous component of ζ_n. To do this, we have to consider the renormalization of appropriate nonlinear Green functions involving the composite operators defined in (31). These are identified and evaluated in section 5. Having calculated the anomalous scaling exponent $-\tau_{np}$ of the pth term in the binomial expansion of $S_n(r)$, in the fourth and final stage of the calculation, we derive a simple algebraic expression for ζ_n by maximizing τ_{np}, with respect to integer values of p, and subtracting this maximum from the Kolmogorov value (3). The results obtained for ζ_n are presented in section 6, where they are shown to be in good agreement with experimental measurements at all orders for which reliable data exists. Finally, the mathematical proofs, deferred during the calculation of the exponents, are presented in sections 7–9, and comprise: (a) the demonstration that sweeping effects can be eliminated by means of the random Galilean transformation of the velocity field; (b) the derivation of the modified quadratic form from the 1-loop expansion; and (c) the derivation of the dominant terms of the OPEs.

3. The structure function expansions

In applying the OPE technique to (1) the first point to appreciate is that the orders $n = 2$, 3 and $\geqslant 4$ require separate treatment. The factor distinguishing S_2 and S_3 from the higher-order S_n is that the latter involve composite operator products, whereas S_2 and S_3 do not. Also, S_3 is exceptional in representing a transition at which corrections to the Kolmogorov exponents (3) change from positive at $n = 2$ to negative at $n \geqslant 4$, with no correction occurring at $n = 3$ in accordance with the known exact scaling law, which is verified, within the present framework, in section 8. This sign change is caused precisely because composite operator products appear in S_n when $n \geqslant 4$.

We begin, therefore, with the relatively straightforward case of S_2. According to (1), we have

$$S_2(r) = 2\big(\langle v^2\rangle - \langle v_+ v_-\rangle\big) \tag{38}$$

which shows that the scaling of S_2 is determined by the behaviour of the operator product v_+v_- as $r \to 0$. The form of its OPE is established in section 9 after the necessary mathematical apparatus has been set up. Its proof is given there to the accuracy of the calculation, ie up to and including terms of order g^2. We shall show that, in the moving frame, the operators which appear in its OPE are: (a) the unit operator I, with constant coefficient $E/3$, where E is the turbulence energy; (b) the dominant longitudinal quadratic composite operator $O_2(\hat{x})$, as given by (31), which gives the leading scaling behaviour; and (c) subdominant operators including all transverse operators and the longitudinal higher-order composite operators $O_s(\hat{x})$. However, we shall only be concerned with the dominant operators and so we write the expansion as

$$v_+v_- = \tfrac{1}{3}EI + C_2(r)O_2(\hat{x}) + \cdots \tag{39}$$

where the dots indicate the additional subdominant terms. The scaling behaviour of this operator product can be found in the usual way from the RG equation satisfied by the leading Wilson coefficient $C_2(r)$ [12].

We start by considering an arbitrary equal time correlation function of order l, given by

$$H_{\alpha_1\ldots\alpha_l}(\hat{x}_1,\ldots,\hat{x}_l) = \big\langle v_{\alpha_1}(\hat{x}_1)\ldots v_{\alpha_l}(\hat{x}_l)\big\rangle. \tag{40}$$

If we insert (39) into this correlation function, we get

$$H_{\alpha_1\ldots\alpha_l}\left(\hat{x}_1,\ldots,\hat{x}_l,\hat{x}+\frac{r}{2}\hat{\imath},\hat{x}-\frac{r}{2}\hat{\imath}\right)=\frac{E}{3}H_{\alpha_1\ldots\alpha_l}(\hat{x}_1,\ldots,\hat{x}_l)$$
$$+C_2(r)Q^{(2)}_{\alpha_1\ldots\alpha_l}(\hat{x}_1,\ldots,\hat{x}_l,\hat{x})+\cdots \tag{41}$$

where, in general, $Q^{(s)}_{\alpha_1\ldots\alpha_l}$ is the inserted correlation function defined by

$$Q^{(s)}_{\alpha_1\ldots\alpha_l}\left(\hat{x}_1,\ldots,\hat{x}_l,\hat{x}\right)=\left\langle v_{\alpha_1}(\hat{x}_1)\ldots v_{\alpha_l}(\hat{x}_l)O_{\rm s}(\hat{x})\right\rangle \tag{42}$$

and $\hat{\imath}$ is a unit vector along the x-axis.

We can deduce the RG equation satisfied by the Wilson coefficient C_2 in (39) from (41), given the RG equations satisfied by $H_{\alpha_1\ldots\alpha_l}$ and $Q^{(2)}_{\alpha_1\ldots\alpha_l}$. To obtain the latter, we need the transformation rule for the equal time generator of these correlation functions, which we denote by $W^{(e)}(\boldsymbol{J},t_{\rm s})$. This follows in a straightforward manner by taking time-independent sources in (37), and integrating with respect to $\omega_{\rm B}$ and $\omega_{\rm R}$, with the $\tilde{\boldsymbol{J}}$ dependence, which is irrelevant here, suppressed. To simplify the result, we shall anticipate the fact, which we demonstrate in section 4, that

$$Z_D=Z_v. \tag{43}$$

We then get

$$W^{(e)}_{\rm R}(\boldsymbol{J},t_{\rm s})=W^{(e)}_{\rm B}\left(\boldsymbol{J},Z_{\rm s}t_{\rm s}\right). \tag{44}$$

According to this relation, the bare and renormalized forms of $H_{\alpha_1\ldots\alpha_l}$ are equal. Hence, when we change the renormalization scale, which we denote by μ, the Fourier transform of $H_{\alpha_1\ldots\alpha_l}$ changes according to the RG equation [12]

$$\mathcal{D}H_{\alpha_1\ldots\alpha_l}=0 \tag{45}$$

where $\mathcal{D}$ is the standard RG operator defined by

$$\mathcal{D}=\mu\frac{\partial}{\partial\mu}+\beta(g)\frac{\partial}{\partial g} \tag{46}$$

with

$$\beta(g)=\mu\frac{{\rm d}g}{{\rm d}\mu}. \tag{47}$$

In the case of $Q^{(s)}_{\alpha_1\ldots\alpha_l}$, we obtain from (42) and (44) the relation

$$(Q^{(s)}_{\alpha_1\ldots\alpha_l})_{\rm R}=Z_{\rm s}(Q^{(s)}_{\alpha_1\ldots\alpha_l})_{\rm B}$$

which leads to the RG equation

$$\mathcal{D}Q^{(s)}_{\alpha_1\ldots\alpha_l}=\gamma_{\rm s}Q^{(s)}_{\alpha_1\ldots\alpha_l} \tag{48}$$

where $\gamma_{\rm s}$ is the anomalous dimension of $O_{\rm s}$ given by

$$\gamma_{\rm s}=\mu\frac{\rm d}{{\rm d}\mu}\log Z_{\rm s}. \tag{49}$$

For ease of notation, we have dropped the suffix R in the RG equations (45) and (48), since we shall always be dealing with relations between renormalized functions.

We now apply the RG operator (46) to the Fourier transform of (41), and make use of (45) and (48), to get

$$0=\left(\mathcal{D}C_2+\gamma_2C_2\right)Q^{(2)}_{\alpha_1\ldots\alpha_l}+\cdots. \tag{50}$$

As this equation holds for arbitrary $Q^{(2)}_{\alpha_1\ldots\alpha_l}$, it follows that

$$\mathcal{D}C_2=-\gamma_2C_2 \tag{51}$$

which is the RG equation satisfied by the Wilson coefficients in (39).

The standard solution of this equation, corresponding to an uv fixed point [12], now gives for the leading term of (39) the scaling behaviour

$$C_2(r) \sim r^{2/3-\gamma_2^*} \tag{52}$$

where the star denotes the fixed point value of (49). This result, in conjunction with (38) and (39), yields the scaling exponent for $S_2(r)$, namely

$$\zeta_2 = \tfrac{2}{3} + \Delta_2 \tag{53}$$

where

$$\Delta_2 = -\gamma_2^*. \tag{54}$$

We shall calculate Δ_2 in section 5.

Consider now the general case for even orders $n = 2m > 2$. Introducing the general composite operator product

$$\Lambda_{ss'}(\hat{x}, r) = O_s\left(\hat{x} + \frac{r}{2}\hat{\imath}\right) O_{s'}\left(\hat{x} - \frac{r}{2}\hat{\imath}\right) \tag{55}$$

and taking advantage of the isotropic symmetry, we can write the binomial expansion of (1) as

$$S_n(r) = n!\left\langle 2\sum_{p=0}^{m-1}(-)^p\,\Lambda_{n-p,p}(\hat{x}, r) + (-)^m\,\Lambda_{m,m}(\hat{x}, r)\right\rangle. \tag{56}$$

We can identify the dominant term of the OPE of $\Lambda_{n-p,p}$ by factoring out the product $(v_+v_-)^p$ and using the fact that, by (39), its expansion begins with the unit operator. We will justify this process in section 9. This implies that the OPE of $\Lambda_{n-p,p}$ itself takes the form

$$\Lambda_{n-p,p}(\hat{x}, r) = C_{p,m-p}(r)\,O_{2(m-p)}(\hat{x}) + \cdots \tag{57}$$

where again the dots indicate subdominant terms. Substituting (57) in (56), we get

$$S_n(r) = n!\left\{2\sum_{p=0}^{m-1}(-)^p C_{p,m-p}(r)\left\langle O_{2(m-p)}(\hat{x})\right\rangle + (-)^m C_{m,m}(r)\right\} + \cdots \tag{58}$$

the averages of the composite operators being independent of $\hat{x}$ for homogeneous isotropic turbulence. To find ζ_n from this expansion, we have to determine which term or terms on the right-hand side yield the negative correction of maximum magnitude to ζ_n^{Kol}. As before, this is deduced from the RG equation for the Wilson coefficient $C_{p,s}$, which we derive next.

We begin by inserting (55) into the general correlation function (40) to obtain the general inserted correlation function

$$R^{(ss')}_{\alpha_1\ldots\alpha_l}(\hat{x}_1, \ldots, \hat{x}_l, \hat{x} + \tfrac{1}{2}r\hat{\imath}, \hat{x} - \tfrac{1}{2}r\hat{\imath}) = \left\langle v_{\alpha_1}(\hat{x}_1)\ldots v_{\alpha_l}(\hat{x}_l)\Lambda_{ss'}(\hat{x}, r)\right\rangle. \tag{59}$$

According to (44) its bare and renormalized forms are connected by the relation

$$\left(R^{(ss')}_{\alpha_1\ldots\alpha_l}\right)_{\mathrm{R}} = Z_s Z_{s'}\left(R^{(ss')}_{\alpha_1\ldots\alpha_l}\right)_{\mathrm{B}}$$

from which it follows that $R^{(ss')}_{\alpha_1\ldots\alpha_l}$ satisfies the RG equation

$$\mathcal{D}R^{(ss')}_{\alpha_1\ldots\alpha_l} = (\gamma_s + \gamma_{s'})\,R^{(ss')}_{\alpha_1\ldots\alpha_l}. \tag{60}$$

Next, we insert the expansion (57) into the general correlation function (40), and use the definitions (42) and (59), to get

$$R^{(n-p,p)}_{\alpha_1\ldots\alpha_l}\left(\hat{x}_1, \ldots, \hat{x}_l, \hat{x} + \frac{r}{2}\hat{\imath}, \hat{x} - \frac{r}{2}\hat{\imath}\right) = C_{p,m-p}(r)\,Q^{(2s)}_{\alpha_1\ldots\alpha_l}\left(\hat{x}_1, \ldots, \hat{x}_l, \hat{x}\right).$$

We then apply the RG operator (46) to the Fourier transform of this equation, and substitute (48) and (60) to obtain

$$Q^{2(m-p)}_{\alpha_1\ldots\alpha_l}\left\{\mathcal{D}C_{p,m-p}+\left(\gamma_{2(m-p)}-\gamma_p-\gamma_{n-p}\right)C_{p,m-p}\right\}+\cdots=0$$

from which it follows that

$$\mathcal{D}C_{p,m-p}=-\left(\gamma_{2(m-p)}-\gamma_p-\gamma_{n-p}\right)C_{p,m-p}. \tag{61}$$

We now invoke the standard solution of (61), applicable at the uv fixed point [12], to obtain the scaling relation

$$C_{p,m-p}(r)\sim r^{n/3-\tau_{np}} \tag{62}$$

where

$$\tau_{np}=\gamma^*_{2(m-p)}-\gamma^*_p-\gamma^*_{n-p}. \tag{63}$$

Upon substituting (62) in (58), it is immediately evident that the scaling exponent of $S_n(r)$ is given by

$$\zeta_n=\frac{n}{3}-\tau_n \tag{64}$$

where

$$\tau_n=\max_p \tau_{np} \qquad \text{for} \quad n=2m>2. \tag{65}$$

Once γ^*_s has been evaluated from (49), at the fixed point, which we do in section 5, it is a simple matter to evaluate τ_n, as we show in section 6.

Odd orders with $n=2m+1>3$ may be treated similarly with minor adjustments to allow for the fact that the expansions involve odd powers. In this case, however, it is immediately evident that the dominant scaling must arise from the Wilson coefficient of the unit operator corresponding to $p=m$, because averaging wipes out other terms by virtue of the fact that $\langle O_{2s+1}\rangle=0$. Hence, we obtain

$$\tau_n=-\left(\gamma^*_m+\gamma^*_{m+1}\right) \qquad \text{for} \quad n=2m+1>3. \tag{66}$$

Again, the justification of the relevant expansions is given in section 9.

4. The linear response

In order to evaluate τ_n, we have to establish that an uv fixed point exists, which entails showing that the RG β function (47) possesses a zero

$$\beta(g_*)=0 \tag{67}$$

at which

$$\frac{\mathrm{d}\beta}{\mathrm{d}g}<0. \tag{68}$$

To do this we must first determine the dependence of the renormalization constants Z_v and Z_D on the renormalization scale μ. We will then verify that (43) holds and use this fact to calculate g_* from Z_v.

4.1. Evaluation of Z_ν

According to the general theory of renormalization [13], the renormalization constant Z_ν has an expansion of the form

$$Z_\nu = 1 + g\, a_{1\nu} \log\left(\frac{\mu}{\kappa}\right) + g^2 \left\{ \frac{a_{1\nu}^2}{2} \log^2\left(\frac{\mu}{\kappa}\right) + a_{2\nu} \log\left(\frac{\mu}{\kappa}\right) \right\} + \cdots . \tag{69}$$

Here κ is the wavenumber cut-off which provides the intermediate regulation of the divergent integrals. In the present case, this is an *ir* wavenumber of the order of L^{-1}, where L is the typical length scale of the large scale flow. Divergences arise in the limit $\kappa \to 0$, corresponding to the inertial range limit $r/L \to 0$. The constants $a_{1\nu}$ and $a_{2\nu}$ will be calculated by eliminating the logarithmic divergences, at 1 and 2-loop orders respectively, from the 1PI Green function $\Gamma_{\alpha\beta}(\hat{k}, \hat{l})$, which is the inverse of the Fourier transform $G_{\alpha\beta}(\hat{k}, \hat{l})$ of the linear response function

$$G_{\alpha\beta}\left(\hat{x}, \hat{x}'\right) = \left\langle \frac{\delta v_\alpha\left(\hat{x}\right)}{\delta f_\beta\left(\hat{x}'\right)} \right\rangle . \tag{70}$$

$\Gamma_{\alpha\beta}$, and the other 1PI functions that we shall require, are generated from the functional K, which is obtained in the usual way by performing a Legendre transformation on $W_c = \log W$, with respect to the sources of the elementary fields, $\boldsymbol{J}$ and $\tilde{\boldsymbol{J}}$, while holding the composite operator sources t_s fixed [7, 14]. The new source fields for K are therefore given by

$$\boldsymbol{u}(\hat{k}) = (2\pi)^4 \frac{\delta W_c}{\mathrm{i}\delta \boldsymbol{J}(-\hat{k})}$$

and

$$\tilde{\boldsymbol{u}}(\hat{k}) = (2\pi)^4 \frac{\delta W_c}{\mathrm{i}\delta \tilde{\boldsymbol{J}}(-\hat{k})}$$

with K itself given in terms of its source fields by

$$K(\boldsymbol{u}, \tilde{\boldsymbol{u}}, t_s) = -W_c + \mathrm{i} \int \left\{ \boldsymbol{J}(-\hat{k}) \cdot \boldsymbol{u}(\hat{k}) + \tilde{\boldsymbol{J}}(-\hat{k}) \cdot \tilde{\boldsymbol{u}}(\hat{k}) \right\} \mathrm{D}\hat{k}.$$

It follows, therefore, that

$$\Gamma_{\alpha\beta}(\hat{k}, \hat{l}) = (2\pi)^8 \frac{\delta^2 K}{\mathrm{i}\delta \tilde{u}_\alpha(\hat{k}) \delta u_\beta(\hat{l})}.$$

Introduction of the reduced forms

$$G_{\alpha\beta}(\hat{k}, \hat{l}) = (2\pi)^4 \delta(\hat{k} + \hat{l}) P_{\alpha\beta}(\boldsymbol{k}) G(\hat{k}) \tag{71}$$

and

$$\Gamma_{\alpha\beta}(\hat{k}, \hat{l}) = (2\pi)^4 \delta(\hat{k} + \hat{l}) P_{\alpha\beta}(\boldsymbol{k}) \Gamma(\hat{k})$$

then leads to the standard relation

$$\Gamma(\hat{k}) = G(\hat{k})^{-1}. \tag{72}$$

We can now use (37) to show that the connection between the bare and renormalized forms is

$$\Gamma_{\mathrm{R}} = Z_\nu \Gamma_{\mathrm{B}} \tag{73}$$

which demonstrates the suitability of $\Gamma(\hat{k})$ as a basis for determining Z_ν.

In carrying out the renormalization of $\Gamma(\hat{k})$ to obtain the coefficients in (69), we choose the normalization point to be $\hat{k} = \hat{m}$, where

$$\hat{m} = (\boldsymbol{m}, \omega_m = 0).$$

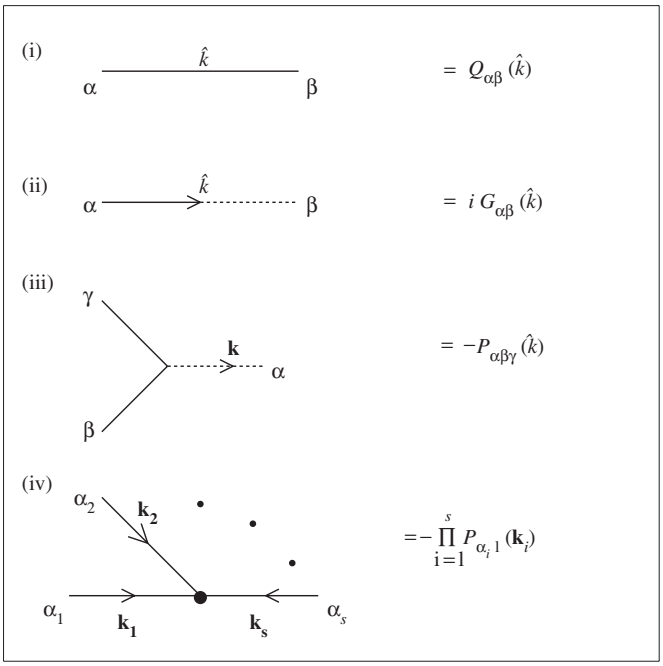

Figure 1. Components of the diagrams: (i) velocity correlator; (ii) linear response function; (iii) NS vertex; (iv) composite operator O_s vertex.

Here $\boldsymbol{m}$ is a fixed vector having a magnitude equal to the renormalization scale μ:

$$|\boldsymbol{m}| = \mu.$$

Since $\mu \gg \kappa$, we have

$$m \gg \kappa. \tag{74}$$

The direction of $\boldsymbol{m}$ need not be specified, because the geometrical factor is contained in $P_{\alpha\beta}(\boldsymbol{m})$ which cancels off. The expansion (69) is used in conjunction with a normalisation condition that sets $\Gamma(\hat{m})$ equal to its tree level value. Thus, from (25) and (72), we have

$$\Gamma(\hat{m}) = \Gamma_0(\hat{m}) = G_0(\hat{m})^{-1} = \tau(\mu)^{-1} \tag{75}$$

and so the 1-loop term satisfies the normalisation condition

$$\Gamma_1(\hat{m}) = 0. \tag{76}$$

The Feynman diagram giving the 1-loop term of $\Gamma_{\alpha\beta}(\hat{m})$ generated by the NS vertex, as given by (20) and (26), is shown in figure 3(i). The standard rules apply to such diagrams with the following assignments, which are shown in figure 1:

(1) External lines represent functional differentiation with respect to $\boldsymbol{u}(\hat{k})$ when continuous, and $\tilde{\boldsymbol{u}}(\hat{k})$, when dotted.The diagram is divided by a factor of i for each differentiation with respect to $\tilde{\boldsymbol{u}}$.

(2) A continuous line linking two vertices denotes the reduced velocity correlation function defined through

$$\left\langle v_\alpha(\hat{k}) v_\beta(\hat{l}) \right\rangle = (2\pi)^4 \delta(\hat{k} + \hat{l})\, Q_{\alpha\beta}(\hat{k})$$

and given by

$$Q_{\alpha\beta}(\hat{k}) = D(k)\left|G(\hat{k})\right|^2 P_{\alpha\beta}(\boldsymbol{k}) \tag{77}$$

$$= \frac{D(k)}{\omega^2 + \sigma(k)^2} P_{\alpha\beta}(\boldsymbol{k}) \tag{78}$$

in which it is convenient to employ the inverse timescale defined by

$$\sigma(k) = \tau(k)^{-1} = \nu k^{2/3}. \tag{79}$$

Also, for ease of notation, we omit zero-order labels in writing down mathematical expressions for the diagrams.

(3) A half dotted/half continuous line connecting two vertices represents i times the zero-order response function

$$G_{\alpha\beta}(\hat{k}) = G(\hat{k}) P_{\alpha\beta}(\boldsymbol{k}) \tag{80}$$

$$= \frac{1}{\mathrm{i}\omega + \sigma(k)} P_{\alpha\beta}(\boldsymbol{k}). \tag{81}$$

(4) The NS vertex with one dotted and two continuous lines represents $-P_{\alpha\beta\gamma}(\boldsymbol{k})$, the vector index α and $\boldsymbol{k}$ being associated with the dotted leg, with $\boldsymbol{k}$ directed away from the node.

Returning now to the 1-loop diagram for $\Gamma_{\alpha\beta}(\hat{m})$, we note that it has a symmetry factor of 1. Hence, it yields a contribution to $\Gamma_1(\hat{m})$ given by

$$P_{\alpha\beta}(\boldsymbol{m})\Gamma_1^{(1)}(\hat{m}) = \int P_{\alpha\gamma\delta}(\boldsymbol{m}) P_{\lambda\nu\beta}(\boldsymbol{m}-\boldsymbol{p}) G_{\gamma\lambda}(\hat{m}-\hat{p}) Q_{\delta\nu}(\hat{p})\,\mathrm{D}\hat{p}.$$

Substituting the zero-order correlator (78) and propagator (81) yields

$$\Gamma_1^{(1)}(\hat{m}) = \tfrac{1}{2}\int A(\boldsymbol{m},\boldsymbol{p}) D(p) I(\boldsymbol{m},\boldsymbol{p})\mathrm{D}\boldsymbol{p} \tag{82}$$

where

$$I(\boldsymbol{m},\boldsymbol{p}) = \frac{1}{2\pi}\int \frac{\mathrm{d}\Omega}{[-\mathrm{i}\Omega + \sigma(|\boldsymbol{m}-\boldsymbol{p}|)][\Omega^2 + \sigma(p)^2]}$$

and

$$A(\boldsymbol{m},\boldsymbol{p}) = P_{\alpha\gamma\delta}(\boldsymbol{m}) P_{\lambda\nu\alpha}(\boldsymbol{m}-\boldsymbol{p}) P_{\gamma\lambda}(\boldsymbol{m}-\boldsymbol{p}) P_{\delta\nu}(\boldsymbol{p}).$$

We can extract the divergence from this integral by expanding its integrand in powers of p/m. This is possible because it emanates from the region $p \sim \kappa$, while from (74) $\kappa \ll m$. The frequency integral I is elementary and, with the approximation $|\boldsymbol{m}-\boldsymbol{p}| \simeq m = \mu$, yields to lowest order

$$I(\boldsymbol{m},\boldsymbol{p}) = \frac{1}{2\sigma(p)[\sigma(p)+\sigma(\mu)]}. \tag{83}$$

$A(\boldsymbol{m},\boldsymbol{p})$ is now the only factor in (82) depending on the direction of $\boldsymbol{p}$. Hence, the integration over the solid angle in (82), together with the approximation $|\boldsymbol{m}-\boldsymbol{p}| \simeq m$, yields the factor

$$\begin{aligned}\int A(\boldsymbol{m},\boldsymbol{p})\,\mathrm{d}o_{\boldsymbol{p}} &= P_{\alpha\gamma\delta}(\boldsymbol{m}) P_{\lambda\nu\alpha}(\boldsymbol{m}) P_{\gamma\lambda}(\boldsymbol{m}) \int P_{\delta\nu}(\boldsymbol{p})\,\mathrm{d}o_{\boldsymbol{p}} \\ &= \frac{8\pi}{3} P_{\alpha\gamma\delta}(\boldsymbol{m}) P_{\lambda\delta\alpha}(\boldsymbol{m}) P_{\gamma\lambda}(\boldsymbol{m}) \\ &= \frac{16\pi m^2}{3} = \frac{16\pi\mu^2}{3}\end{aligned} \tag{84}$$

where we have used the definitions (16) and (17).

Substituting (28), (83), and (84) in (82), and using the definitions (36) and (79), leads to

$$\Gamma_1^{(1)}(\hat{m}) = g\sigma(k)^3 \int_{p>\kappa} \frac{\mathrm{d}p}{p\sigma(p)[\sigma(p)+\sigma(\mu)]}.$$

Next we change from an integration over wavenumber p to an integration over the non-dimensional variable x defined by

$$x = \frac{\sigma(p)}{\sigma(\mu)}. \tag{85}$$

After making use of (79), we obtain

$$\Gamma_1^{(1)}(\hat{m}) = \tfrac{3}{2} g\tau(\mu)^{-1} I_0(\varepsilon) \tag{86}$$

where

$$I_0(\varepsilon) = \int_\varepsilon^\infty \frac{\mathrm{d}x}{x^2(x+1)} \tag{87}$$

in which the lower limit of integration is

$$\varepsilon = \frac{\tau(\mu)}{\tau(\kappa)}. \tag{88}$$

Evaluation of (87) is trivial and yields the divergent terms

$$I_0(\varepsilon) = \log\varepsilon + \frac{1}{\varepsilon} \tag{89}$$

giving

$$\Gamma_1^{(1)}(\hat{m}) = \frac{3}{2}\frac{g}{\tau(\mu)}\log\varepsilon + \frac{3}{2}\frac{g}{\tau(\mu)}\frac{1}{\varepsilon}. \tag{90}$$

To this we must add the contributions from the sweeping interaction term (30) and the counterterm (33). In section 7, we will show that the 1-loop term arising from the sweeping interaction cancels the power divergence in (90), and so this term may be omitted from $\Gamma_1^{(1)}(\hat{m})$. This leaves the logarithmic divergence which, on making use of (88) and (79), becomes

$$\Gamma_1^{(1)}(\hat{m}) = -\tau(\mu)^{-1} g \log\left(\frac{\mu}{\kappa}\right). \tag{91}$$

The counterterm vertex shown in figure 2(i) contributes the term $P_{\alpha\beta}(\boldsymbol{m})\,\Gamma_1^{(2)}(\hat{m})$ where

$$\Gamma_1^{(2)}(\hat{m}) = \Delta Z_\nu \tau(\mu)^{-1} = a_{1\nu}\tau(\mu)^{-1} g \log\left(\frac{\mu}{\kappa}\right). \tag{92}$$

But, from the normalization condition (76), we have

$$\Gamma_1^{(1)}(\hat{m}) + \Gamma_1^{(2)}(\hat{m}) = 0$$

which, upon substituting (91) and (92), yields

$$a_{1\nu} = 1. \tag{93}$$

The other constant in (69), $a_{2\nu}$, is obtained from the 2-loop term of $\Gamma_{\alpha\beta}(\hat{m})$, namely $P_{\alpha\beta}(\boldsymbol{m})\Gamma_2(\hat{m})$. At the normalization point it must satisfy the condition

$$\Gamma_2(\hat{m}) = 0 \tag{94}$$

by virtue of (76). There are nine possible Feynman diagrams for $\Gamma_{\alpha\beta}(\hat{m})$ containing two loops. But, for reasons discussed fully below, only two of them yield divergences after integration

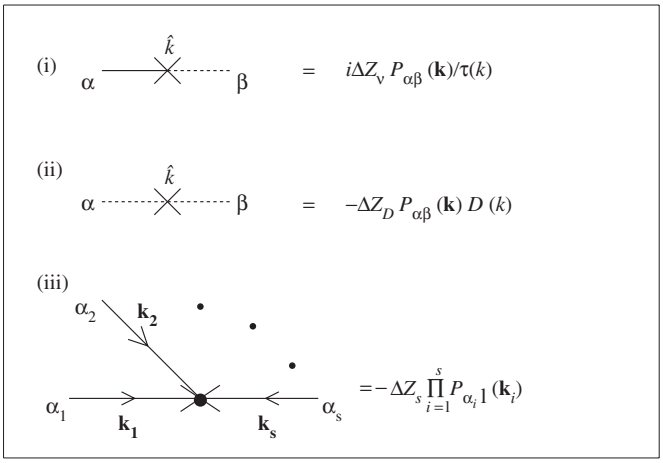

Figure 2. Counterterm vertices associated with the renormalization of the elementary fields and the composite operators.

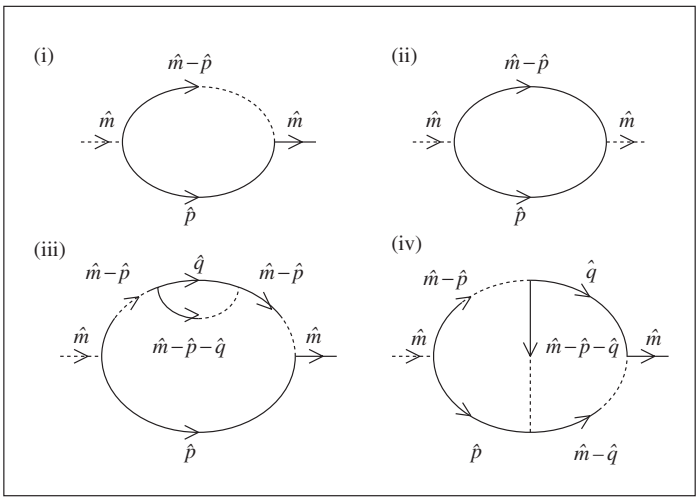

Figure 3. The 1PI Feynman diagrams evaluated in section 4 for (i) Γ_1, (ii) Π_1, (iii) and (iv) Γ_2.

over the solid angles. They are shown in figures 3(iii) and (iv). Their symmetry factors are 1 and they contribute the terms

$$P_{\alpha\beta}(\boldsymbol{m})\Gamma_2^{(1)}(\hat{m}) = -\int \mathrm{D}\hat{p}\,\mathrm{D}\hat{q}\; Q_{\delta\epsilon}(\hat{p})Q_{\lambda\rho}(\hat{q})$$
$$\times G_{\kappa\gamma}(\hat{m}-\hat{p})G_{\nu\sigma}(\hat{m}-\hat{p}-\hat{q})G_{\tau\mu}(\hat{m}-\hat{p})$$
$$\times P_{\alpha\gamma\delta}(\boldsymbol{m})P_{\mu\beta\epsilon}(\boldsymbol{m}-\boldsymbol{p})P_{\kappa\lambda\nu}(\boldsymbol{m}-\boldsymbol{p})P_{\sigma\rho\tau}(\boldsymbol{m}-\boldsymbol{p}-\boldsymbol{q}) \tag{95}$$

and

$$P_{\alpha\beta}(\boldsymbol{m})\Gamma_2^{(2)}(\hat{m}) = -\int \mathrm{D}\hat{p}\,\mathrm{D}\hat{q}\; Q_{\delta\sigma}(\hat{p})Q_{\lambda\mu}(\hat{q})$$
$$\times G_{\kappa\gamma}(\hat{m}-\hat{p})G_{\varrho\nu}(\hat{m}-\hat{p}-\hat{q})G_{\epsilon\tau}(\hat{m}-\hat{q}) \tag{96}$$
$$\times P_{\alpha\gamma\delta}(\boldsymbol{m})P_{\epsilon\mu\beta}(\boldsymbol{m}-\boldsymbol{q})P_{\kappa\lambda\nu}(\boldsymbol{m}-\boldsymbol{p})P_{\varrho\sigma\tau}(\boldsymbol{m}-\boldsymbol{p}-\boldsymbol{q}). \tag{97}$$

Evaluation of these 2-loop integrals proceeds essentially as just described for the 1-loop case. Consider first (95). Substitution of (78) and (81) gives

$$\Gamma_2^{(1)}(\hat{m}) = -\tfrac{1}{2}\int A(\boldsymbol{m},\boldsymbol{p},\boldsymbol{q})D(p)D(q)I(\boldsymbol{m},\boldsymbol{p},\boldsymbol{q})\,\mathrm{D}\boldsymbol{p}\,\mathrm{D}\boldsymbol{q} \tag{98}$$

where

$$A(\boldsymbol{m},\boldsymbol{p},\boldsymbol{q}) = P_{\alpha\gamma\delta}(\boldsymbol{m})P_{\gamma\lambda\nu}(\boldsymbol{m}-\boldsymbol{p})P_{\nu\rho\tau}(\boldsymbol{m}-\boldsymbol{p}-\boldsymbol{q})P_{\tau\alpha\epsilon}(\boldsymbol{m}-\boldsymbol{p})P_{\delta\epsilon}(\boldsymbol{p})P_{\lambda\rho}(\boldsymbol{q})$$

and where I is the double frequency integral given by

$$I(\boldsymbol{m},\boldsymbol{p},\boldsymbol{q}) = \frac{1}{(2\pi)^2}\int \left|G(\hat{p})G(\hat{q})\right|^2 G(\hat{m}-\hat{p})^2 G(\hat{m}-\hat{p}-\hat{q})\,\mathrm{d}\Omega_p\,\mathrm{d}\Omega_q. \tag{99}$$

We extract the divergences from (98), by expanding its integrand in powers of both p/m and q/m. Substituting (81) in (99), and using the approximations $|\boldsymbol{m}-\boldsymbol{p}| \simeq m = \mu$, $|\boldsymbol{m}-\boldsymbol{q}| \simeq m = \mu$ and $|\boldsymbol{m}-\boldsymbol{p}-\boldsymbol{q}| \simeq m = \mu$, we get

$$I(\boldsymbol{m},\boldsymbol{p},\boldsymbol{q}) = \frac{1}{(2\pi)^2}\int \frac{\mathrm{d}\Omega_p\,\mathrm{d}\Omega_q}{[\Omega_p^2+\sigma(p)^2][\Omega_q^2+\sigma(q)^2][-\mathrm{i}\Omega_p+\sigma(\mu)]^2[-\mathrm{i}(\Omega_p+\Omega_q)+\sigma(\mu)]}$$

yielding

$$I(\boldsymbol{m},\boldsymbol{p},\boldsymbol{q}) = \frac{1}{4\sigma(p)\sigma(q)[\sigma(p)+\sigma(\mu)]^2[\sigma(p)+\sigma(q)+\sigma(\mu)]}. \tag{100}$$

Integration over the solid angles in (98) now involves only $A(\boldsymbol{m},\boldsymbol{p},\boldsymbol{q})$ and yields the factor

$$\begin{aligned}\int A(\boldsymbol{m},\boldsymbol{p},\boldsymbol{q})\,\mathrm{d}o_{\boldsymbol{p}}\,\mathrm{d}o_{\boldsymbol{q}} &= P_{\alpha\gamma\delta}(\boldsymbol{m})P_{\gamma\lambda\nu}(\boldsymbol{m})P_{\nu\rho\tau}(\boldsymbol{m})P_{\tau\alpha\epsilon}(\boldsymbol{m})\int P_{\delta\epsilon}(\boldsymbol{p})P_{\lambda\rho}(\boldsymbol{q})\,\mathrm{d}o_{\boldsymbol{p}}\,\mathrm{d}o_{\boldsymbol{q}}\\ &= 2\left(\frac{8\pi\mu^2}{3}\right)^2.\end{aligned} \tag{101}$$

Substituting (28), (100) and (101), in (98), and using (36) and (79), we obtain, to lowest order,

$$\Gamma_2^{(1)}(\hat{m}) = -g^2\sigma(\mu)^6\int_{p,q>\kappa}\frac{\mathrm{d}p\,\mathrm{d}q}{pq\sigma(p)\sigma(q)[\sigma(p)+\sigma(\mu)]^2[\sigma(p)+\sigma(q)+\sigma(\mu)]}.$$

Next, we change to non-dimensional variables of integration defined by

$$x = \frac{\sigma(p)}{\sigma(\mu)} \qquad \text{and} \qquad y = \frac{\sigma(q)}{\sigma(\mu)} \tag{102}$$

to get

$$\Gamma_2^{(1)}(\hat{m}) = -\tfrac{9}{4}g^2\tau(\mu)^{-1}I_1(\varepsilon) \tag{103}$$

where

$$I_1(\varepsilon) = \int_\varepsilon^\infty\int_\varepsilon^\infty \frac{1}{x^2y^2(1+x)^2(1+x+y)}\,\mathrm{d}x\,\mathrm{d}y. \tag{104}$$

Extracting the divergent terms from this integral for small ε now gives

$$I_1(\varepsilon) = I_1^{(l)}(\varepsilon) + I_1^{(p)}(\varepsilon) \tag{105}$$

where $I_1^{(l)}$ consists of the purely logarithmic divergences

$$I_1^{(l)}(\varepsilon) = \tfrac{16}{3}\log\varepsilon + 4\log^2\varepsilon$$

while $I_1^{(p)}$ comprises the power divergences

$$I_1^{(p)}(\varepsilon) = \frac{1}{\varepsilon^2} + \frac{5}{2}\frac{1}{\varepsilon} + \frac{4}{\varepsilon}\log\varepsilon. \tag{106}$$

As with the 1-loop term, it will be shown in section 7 that $I_1^{(p)}$ is exactly cancelled by the corresponding 2-loop terms arising from the sweeping interaction (30). So we can omit $I_1^{(p)}$ from I_1. Furthermore, for the calculation of the coefficient $a_{2\nu}$ in (69), we require only the singly logarithmic divergence, as in standard renormalization calculations [8]. So we can also remove the $\log^2$ term from $I_1^{(l)}$. Thus, we are left finally with

$$I_1(\varepsilon) = \tfrac{16}{3}\log\varepsilon$$

and (103) yields

$$\Gamma_2^{(1)}(\hat{m}) = 8g^2\tau(\mu)^{-1}\log\left(\frac{\mu}{\kappa}\right) \tag{107}$$

where we have used (79).

Similarly, for $\Gamma_2^{(2)}(\hat{m})$, we get from (97)

$$\Gamma_2^{(2)}(\hat{m}) = -\tfrac{1}{2}\int A(\boldsymbol{m},\boldsymbol{p},\boldsymbol{q})D(p)D(q)I(\boldsymbol{m},\boldsymbol{p},\boldsymbol{q})\,\mathrm{D}\boldsymbol{p}\,\mathrm{D}\boldsymbol{q}$$

where

$$A(\boldsymbol{m},\boldsymbol{p},\boldsymbol{q}) = P_{\alpha\beta\gamma}(\boldsymbol{m})P_{\gamma\lambda\mu}(\boldsymbol{m}-\boldsymbol{p})P_{\tau\nu\alpha}(\boldsymbol{m}-\boldsymbol{p})P_{\mu\sigma\tau}(\boldsymbol{m}-\boldsymbol{p}-\boldsymbol{q})P_{\beta\sigma}(\boldsymbol{p})P_{\lambda\nu}(\boldsymbol{q})$$

and

$$I(\boldsymbol{m},\boldsymbol{p},\boldsymbol{q}) = \frac{1}{(2\pi)^2}\int \left|G(\hat{p})G(\hat{q})\right|^2 G(\hat{m}-\hat{p})G(\hat{m}-\hat{q})G(\hat{m}-\hat{p}-\hat{q})\,\mathrm{d}\Omega_p\,\mathrm{d}\Omega_q.$$

Using the approximation $p, q \ll m$ as before, we find that the result (101) again applies to the angular integrations, while the frequency integral yields

$$I(\boldsymbol{m},\boldsymbol{p},\boldsymbol{q}) = \frac{1}{4\sigma(p)\sigma(q)[\sigma(p)+\sigma(\mu)][\sigma(q)+\sigma(\mu)][\sigma(p)+\sigma(q)+\sigma(\mu)]}$$

leading to

$$\Gamma_2^{(2)}(\hat{m}) = -g^2\sigma(\mu)^6\int_{p,q>\kappa}\frac{\mathrm{d}p\,\mathrm{d}q}{pq\sigma(p)\sigma(q)[\sigma(p)+\sigma(\mu)][\sigma(q)+\sigma(\mu)][\sigma(p)+\sigma(q)+\sigma(\mu)]}.$$

Changing to the non-dimensional variables (102) now gives

$$\Gamma_2^{(2)}(\hat{m}) = -\tfrac{9}{4}g^2\tau(\mu)^{-1}I_2(\varepsilon) \tag{108}$$

where

$$I_2(\varepsilon) = \int_\varepsilon^\infty\int_\varepsilon^\infty \frac{\mathrm{d}x\,\mathrm{d}y}{x^2y^2(1+x)(1+y)(1+x+y)}. \tag{109}$$

Extraction of the divergent terms in this case yields

$$I_2(\varepsilon) = I_2^{(l)}(\varepsilon) + I_2^{(p)}(\varepsilon) \tag{110}$$

where

$$I_2^{(l)}(\varepsilon) = 7\log\varepsilon + 5\log^2\varepsilon$$

and

$$I_2^{(p)}(\varepsilon) = \frac{1}{\varepsilon^2} + \frac{2}{\varepsilon} + \frac{4}{\varepsilon}\log\varepsilon. \tag{111}$$

Again, we will show in section 7 that the power divergences are exactly cancelled by the corresponding 2-loop terms arising from the sweeping interaction (30). So we can omit $I_2^{(p)}$ from I_2. Since we need only retain the singly logarithmic divergence for the calculation of $a_{2\nu}$, we are left with

$$I_2(\varepsilon) = 7\log\varepsilon$$

and (108) yields

$$\Gamma_2^{(2)}(\hat{m}) = \frac{21}{2}\tau(\mu)^{-1}g^2\log\left(\frac{\mu}{\kappa}\right). \tag{112}$$

To the two contributions (107) and (112) to $\Gamma_2(\hat{m})$, we must add the counterterm, which, by analogy with (92), takes the form

$$\Gamma_2^{(3)}(\hat{m}) = a_{2v}g^2\tau(\mu)^{-1}\log\left(\frac{\mu}{\kappa}\right). \tag{113}$$

Thus, the normalization condition (94) becomes

$$\Gamma_2^{(1)}(\hat{m}) + \Gamma_2^{(2)}(\hat{m}) + \Gamma_2^{(3)}(\hat{m}) = 0.$$

Substitution of (107), (112) and (113) in this condition now yields

$$a_{2v} = -\tfrac{37}{2}. \tag{114}$$

Note from (85) and (110) that the sum of the 2-loop divergences is

$$I_1 + I_2 = \frac{37}{2}\log\varepsilon + 9\log^2\varepsilon + \frac{9}{2}\frac{1}{\varepsilon} + \frac{2}{\varepsilon^2} + 8\frac{\log\varepsilon}{\varepsilon}. \tag{115}$$

Finally, we explain why the 2-loop topologies, which have been discarded in calculating Γ, do not contribute to a_{2v}. As we shall explain further in section 7, divergences arise in these diagrams when it is possible for one or more soft wavevectors (i.e. values of p and/or $q \ll m$) to flow through a correlator. However, if this entails the flow of some or all of these wavevectors through the active (i.e. dotted) leg of the NS vertex, then the logarithmic divergence will be suppressed by the extra powers of p and/or q. In the case of the 2-loop diagrams which we have just calculated, the external hard wavevector $\hat{m}$ flows through the active legs of all vertices, so no suppression occurs. However, in the case of the remaining topologies, at least one soft wavevector flowing through a correlator must also flow through the active leg of a NS vertex. For the four remaining 2-loop topologies containing vertex corrections, the divergence is suppressed individually for each diagram, after integration over the solid angles. For the three remaining 2-loop diagrams containing insertions of the 1-loop diagrams (i) and (ii) of figure 3, suppression results after integrating over the solid angles and summing over the diagrams, the overall cancellation being related to the fact that the coefficients a_{1v} and a_{1D} associated with the two types of insertion are equal, as we show shortly. Likewise the four 1-loop diagrams containing the counterterm vertices yield no net contribution to a_{2v}, although they do contribute a $\log^2(\varepsilon)$ term to Z_v, such that the overall coefficient of its $\log^2(\varepsilon)$ term is as determined by the 1-loop expansion, in accordance with (69).

4.2. Evaluation of Z_D

The calculation of the renormalization constant Z_D proceeds along similar lines to the calculations just described for Z_v, although the detail is substantially different. The expansion of Z_D, of course, takes the same form as (69), namely

$$Z_D = 1 + g\,a_{1D}\log\left(\frac{\mu}{\kappa}\right) + g^2\left\{\frac{a_{1D}^2}{2}\log^2\left(\frac{\mu}{\kappa}\right) + a_{2D}\log\left(\frac{\mu}{\kappa}\right)\right\} + \cdots. \tag{116}$$

We shall show that $a_{1D} = a_{1v}$ and $a_{2D} = a_{2v}$, thereby verifying that the condition (43) is satisfied to 2-loop order.

Here the relevant 1PI function is the correlation function given by

$$\Pi_{\alpha\beta}(\hat{k},\hat{l}) = (2\pi)^8\,\frac{\delta^2 K}{\mathrm{i}\delta\tilde{u}_\alpha\,\mathrm{i}\delta\tilde{u}_\beta}$$

which is readily shown to be related to the velocity correlation function $Q_{\alpha\beta}(\hat{k}, \hat{l})$ by [14]

$$\Pi_{\alpha\beta}(\hat{k}, \hat{l}) = \int \Gamma_{\alpha\lambda}(\hat{k}, \hat{p})\Gamma_{\beta\mu}(\hat{l}, \hat{q})Q_{\lambda\mu}(\hat{p}, \hat{q})\,\mathrm{d}\hat{p}\,\mathrm{d}\hat{q}.$$

Substituting the reduced forms

$$\Pi_{\alpha\beta}(\hat{k}, \hat{l}) = (2\pi)^4\delta(\hat{k} + \hat{l})P_{\alpha\beta}(\boldsymbol{k})\Pi(\hat{k})$$

and

$$Q_{\alpha\beta}(\hat{k}, \hat{l}) = (2\pi)^4\delta(\hat{k} + \hat{l})\,P_{\alpha\beta}(\boldsymbol{k})Q(\hat{k})$$

we get

$$\Pi(\hat{k}) = \left|\Gamma(\hat{k})\right|^2 Q(\hat{k}).$$

From this result and (37) and (72), we find that the bare and renormalized forms of Π are related by

$$\Pi_{\mathrm{R}} = Z_D\Pi_{\mathrm{B}}$$

which confirms that $\Pi(\hat{k})$ is the appropriate 1PI function to use for calculating Z_D.

The normalization condition is again chosen to be consistent with the tree level approximation, as implied in (116). That is, we set

$$\Pi(\hat{m}) = \Pi_0(\hat{m}) = D\,(\mu) \tag{117}$$

so that the 1-loop term satisfies the normalization condition

$$\Pi_1(\hat{m}) = 0. \tag{118}$$

The 1-loop Feynman diagram for $\Pi_{\alpha\beta}(\hat{m})$ is shown in figure 3(ii). It has a symmetry factor of $1/2$, and makes a contribution to $\Pi_1(\hat{m})$ which is given by

$$P_{\alpha\beta}(\boldsymbol{m})\Pi_1^{(1)}(\hat{m}) = \tfrac{1}{2}\int P_{\alpha\gamma\delta}(\boldsymbol{m})P_{\beta\lambda\nu}(\boldsymbol{m})Q_{\gamma\lambda}(\hat{p})Q_{\delta\nu}(\hat{m} - \hat{p})\,\mathrm{D}\hat{p}.$$

Substituting (78) yields

$$\Pi_1^{(1)}(\hat{m}) = \tfrac{1}{4}\int A(\boldsymbol{m}, \boldsymbol{p})D(p)D(|\boldsymbol{m} - \boldsymbol{p}|)I(\boldsymbol{m}, \boldsymbol{p})\,\mathrm{D}\boldsymbol{p} \tag{119}$$

where

$$I(\boldsymbol{m}, \boldsymbol{p}) = \frac{1}{2\pi}\int \frac{\mathrm{d}\Omega}{[\Omega^2 + \sigma(|\boldsymbol{m} - \boldsymbol{p}|)^2][\Omega^2 + \sigma(p)^2]}$$

and

$$A(\boldsymbol{m}, \boldsymbol{p}) = P_{\alpha\gamma\delta}(\boldsymbol{m})P_{\alpha\lambda\nu}(\boldsymbol{m})P_{\gamma\lambda}(\boldsymbol{p})P_{\delta\nu}(\boldsymbol{m} - \boldsymbol{p}).$$

The frequency integral can be carried out exactly to give

$$I(\boldsymbol{m}, \boldsymbol{p}) = \frac{1}{2\sigma(p)\sigma(|\boldsymbol{m} - \boldsymbol{p}|)[\sigma(p) + \sigma(|\boldsymbol{m} - \boldsymbol{p}|)]}.$$

In extracting the logarithmic singularity from (119), we must take into account the fact that the symmetry of the integrand results in singularities of equal strength at both $p \sim \kappa$, and $|\boldsymbol{p} - \boldsymbol{m}| \sim \kappa$, the effect of which compensates for the symmetry factor. This follows by re-writing (119) in the form

$$\Pi_1^{(1)}(\hat{m}) = \frac{1}{4}\int A(\boldsymbol{m}, \boldsymbol{p})\frac{1}{D(p)^{-1} + D(|\boldsymbol{m} - \boldsymbol{p}|)^{-1}}[D(p) + D(|\boldsymbol{m} - \boldsymbol{p}|)]I(\boldsymbol{m}, \boldsymbol{p})\,\mathrm{D}\boldsymbol{p}$$

and then applying the transformation $\boldsymbol{p} \to \boldsymbol{m} - \boldsymbol{p}$ to the second term between the braces. Since both $A(\boldsymbol{m}, \boldsymbol{p})$ and $I(\boldsymbol{m}, \boldsymbol{p})$ are symmetric under this transformation, we get

$$\Pi_1^{(1)}(\hat{m}) = \frac{1}{2} \int A(\boldsymbol{m}, \boldsymbol{p}) \frac{1}{D(p)^{-1} + D(|\boldsymbol{m} - \boldsymbol{p}|)^{-1}} D(p) I(\boldsymbol{m}, \boldsymbol{p}) \, \mathrm{D}\boldsymbol{p}. \quad (120)$$

In this latter form, the divergences arise only from the region $p \sim \kappa$, and so we can evaluate the integral by expanding its integrand in powers of p/m as before. In this approximation we have

$$I(\boldsymbol{m}, \boldsymbol{p}) = \frac{1}{2\sigma(p)[\sigma(p) + \sigma(\mu)]}$$

and

$$\left[D(p)^{-1} + D(|\boldsymbol{m} - \boldsymbol{p}|)^{-1}\right]^{-1} \simeq D(\mu)$$

while the angular integration gives

$$\int A(\boldsymbol{m}, \boldsymbol{p}) \, \mathrm{d}o_{\boldsymbol{p}} = \frac{8\pi}{3} P_{\alpha\gamma\delta}(\boldsymbol{m}) P_{\alpha\gamma\nu}(\boldsymbol{m}) P_{\delta\nu}(\boldsymbol{m}) = \frac{16\pi\mu^2}{3}.$$

Substituting these results in (120), and using (79) and (36), we obtain

$$\Pi_1^{(1)}(\hat{m}) = D(\mu) g \sigma(k)^2 \int_{p>\kappa} \frac{\mathrm{d}p}{p\sigma(p)[\sigma(p) + \sigma(\mu)]}$$

which, after changing to the non-dimensional variable (85), becomes

$$\Pi_1^{(1)}(\hat{m}) = \tfrac{3}{2} D(\mu) g I_0(\varepsilon) \quad (121)$$

where I_0 is the integral (87) obtained for $\Gamma_1^{(1)}(\hat{m})$.

It follows from (75), (86), (117) and (121) that the ratios of the divergences of the 1-loop term to the tree level term for the two 1PI functions, from which Z_D and Z_ν are calculated, are equal at the normalization point and given by

$$\frac{\Pi_1^{(1)}(\hat{m})}{\Pi_0(\hat{m})} = \frac{\Gamma_1^{(1)}(\hat{m})}{\Gamma_0(\hat{m})} = \frac{3}{2} g I_0(\varepsilon). \quad (122)$$

Thus, they have identical divergences arising from the NS vertex. In particular, the coefficient a_{1D} in the expansion of Z_D must equal the corresponding coefficient $a_{1\nu}$ for Z_ν. Indeed, from (87) and (121), we obtain a logarithmic divergence

$$\Pi_1^{(1)}(\hat{m}) = -D(\mu) g \log\left(\frac{\mu}{\kappa}\right) \quad (123)$$

while the Z_D counterterm, which is shown in figure 2(ii), contributes a term to $\Pi_1(\hat{m})$ given by

$$\Pi_1^{(2)}(\hat{m}) = \Delta Z_D D(\mu) = a_{1D} D(\mu) \, g \log\left(\frac{\mu}{\kappa}\right). \quad (124)$$

But, from the normalization condition (118), we have

$$\Pi_1^{(1)}(\hat{m}) + \Pi_1^{(2)}(\hat{m}) = 0$$

and substitution of (123) and (124) leads to

$$a_{1D} = 1$$

which equals the value (93) obtained for $a_{1\nu}$.

We demonstrate next that the same results are obtained at 2-loop order. Here we find that there are five possible topologies for the Feynman diagrams. Four of these contribute divergences after integration over the solid angles, the fifth giving zero. They are shown in

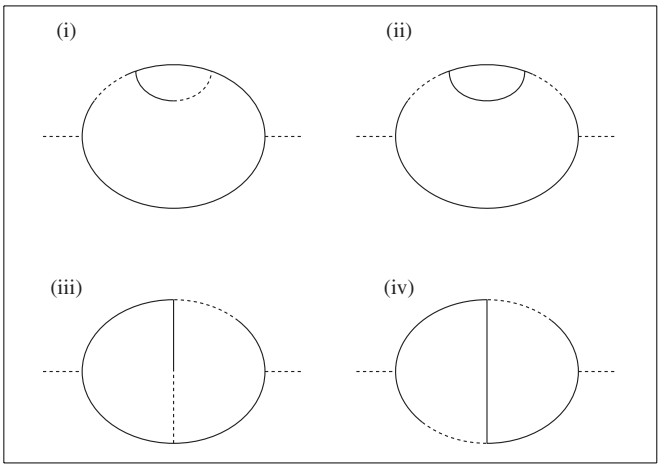

Figure 4. The 1PI Feynman diagrams evaluated in section 4 for Π_2.

figure 4. Their symmetry factors are 2, 1/2, 2 and 1, respectively. In diagram(ii) there is a doubling of the strength of the singularity at $p, q \sim \kappa$ associated with the insertion of the $\Pi_1^{(1)}$ loop discussed above, which offsets its symmetry factor of 1/2. The diagrams generated by rotating diagrams (i) and (iii) about a vertical axis have been allowed for by doubling the symmetry factors, as indicated. Each diagram contributes a term of the form

$$\Pi_2^{(s)}(\hat{m}) = -\tfrac{9}{4} D(\mu) g^2 J_s(\varepsilon) \qquad \text{with} \quad s = 1, \ldots, 4 \tag{125}$$

in which the final factor is found using the procedure employed for the earlier cases.

Specifically, for diagram 4(i), we get

$$\Pi_2^{(1)}(\hat{m}) = -\int A(\boldsymbol{m}, \boldsymbol{p}, \boldsymbol{q}) D(p) D(q) D(|\boldsymbol{m} - \boldsymbol{p}|) I(\boldsymbol{m}, \boldsymbol{p}, \boldsymbol{q}) \, \mathrm{D}\boldsymbol{p} \, \mathrm{D}\boldsymbol{q}$$

where

$$I(\boldsymbol{m}, \boldsymbol{p}, \boldsymbol{q}) = \frac{1}{(2\pi)^2} \int \left| G(\hat{p}) G(\hat{q}) G(\hat{m} - \hat{p}) \right|^2 G(\hat{m} - \hat{p}) G(\hat{m} - \hat{p} - \hat{q}) \, \mathrm{d}\Omega_p \, \mathrm{d}\Omega_q$$

and

$$A(\boldsymbol{m}, \boldsymbol{p}, \boldsymbol{q}) = P_{\alpha\gamma\delta}(\boldsymbol{m}) P_{\alpha\kappa\sigma}(\boldsymbol{m}) P_{\tau\gamma\mu}(\boldsymbol{m} - \boldsymbol{p} - \boldsymbol{q}) P_{\rho\tau\lambda}(\boldsymbol{m} - \boldsymbol{p}) P_{\kappa\gamma}(\boldsymbol{m} - \boldsymbol{p}) P_{\delta\sigma}(\boldsymbol{p}) P_{\lambda\mu}(\boldsymbol{q})$$

which leads to

$$J_1(\varepsilon) = \int_\varepsilon^\infty \int_\varepsilon^\infty \frac{x(x+1) + (2+x)(2+y)}{x^2 y^2 (1+x)^2 (1+x+y)(2+y)} \, \mathrm{d}x \, \mathrm{d}y.$$

Similarly, for diagram 4(ii), we get

$$\Pi_2^{(2)}(\hat{m}) = -\tfrac{1}{4} \int A(\boldsymbol{m}, \boldsymbol{p}, \boldsymbol{q}) D(p) D(q) D(|\boldsymbol{m} - \boldsymbol{p} - \boldsymbol{q}|) I(\boldsymbol{m}, \boldsymbol{p}, \boldsymbol{q}) \, \mathrm{D}\boldsymbol{p} \, \mathrm{D}\boldsymbol{q}$$

where

$$I(\boldsymbol{m}, \boldsymbol{p}, \boldsymbol{q}) = \frac{1}{(2\pi)^2} \int \left| G(\hat{p}) G(\hat{q}) G(\hat{m} - \hat{p}) G(\hat{m} - \hat{p} - \hat{q}) \right|^2 \, \mathrm{d}\Omega_p \, \mathrm{d}\Omega_q$$

and

$$A(\boldsymbol{m}, \boldsymbol{p}, \boldsymbol{q}) = P_{\alpha\beta\gamma}(\boldsymbol{m}) P_{\alpha\delta\lambda}(\boldsymbol{m}) P_{\beta\mu\nu}(\boldsymbol{m} - \boldsymbol{p}) P_{\delta\sigma\rho}(\boldsymbol{m} - \boldsymbol{p}) P_{\gamma\lambda}(\boldsymbol{p}) P_{\nu\rho}(\boldsymbol{q}) P_{\mu\sigma}(\boldsymbol{m} - \boldsymbol{p} - \boldsymbol{q})$$

which leads to

$$J_2(\varepsilon) = \int_\varepsilon^\infty \int_\varepsilon^\infty \frac{2+x+y}{x^2y^2\,(1+x)\,(1+x+y)\,(2+y)}\,\mathrm{d}x\,\mathrm{d}y.$$

Again, for diagram 4(iii), we get

$$\Pi_2^{(3)}(\hat{m}) = -\int A(\boldsymbol{m},\boldsymbol{p},\boldsymbol{q})D(p)D(q)D(|\boldsymbol{m}-\boldsymbol{p}|)I(\boldsymbol{m},\boldsymbol{p},\boldsymbol{q})\,\mathrm{D}\boldsymbol{p}\,\mathrm{D}\boldsymbol{q}$$

where

$$I(\boldsymbol{m},\boldsymbol{p},\boldsymbol{q}) = \frac{1}{(2\pi)^2}\int \left|G(\hat{p})G(\hat{q})G(\hat{m}-\hat{p})\right|^2 G(-\hat{m}+\hat{q})G(-\hat{m}+\hat{p}+\hat{q})\,\mathrm{d}\Omega_p\,\mathrm{d}\Omega_q$$

and

$$A(\boldsymbol{m},\boldsymbol{p},\boldsymbol{q}) = P_{\alpha\beta\gamma}(\boldsymbol{m})P_{\alpha\delta\lambda}(\boldsymbol{m})P_{\tau\nu\rho}(\boldsymbol{m}-\boldsymbol{p}-\boldsymbol{q})P_{\delta\sigma\tau}(\boldsymbol{m}-\boldsymbol{q})P_{\nu\gamma}(\boldsymbol{m}-\boldsymbol{p})P_{\beta\sigma}(\boldsymbol{p})P_{\lambda\rho}(\boldsymbol{q})$$

which leads to

$$J_3(\varepsilon) = 2\int_\varepsilon^\infty \int_\varepsilon^\infty \frac{x(x+1)+(2+x)(2+y)}{x^2y^2\,(1+x)\,(1+x+y)\,(1+y)(2+y)}\,\mathrm{d}x\,\mathrm{d}y. \tag{126}$$

Finally, for diagram 4(iv), we get

$$\Pi_2^{(4)}(\hat{m}) = \tfrac{1}{2}\int A(\boldsymbol{m},\boldsymbol{p},\boldsymbol{q})D(p)D(q)D(|\boldsymbol{m}-\boldsymbol{p}-\boldsymbol{q}|)I(\boldsymbol{m},\boldsymbol{p},\boldsymbol{q})\,\mathrm{D}\boldsymbol{p}\,\mathrm{D}\boldsymbol{q}$$

where

$$I(\boldsymbol{m},\boldsymbol{p},\boldsymbol{q}) = \frac{1}{(2\pi)^2}\int \left|G(\hat{p})G(\hat{q})G(\hat{m}-\hat{p}-\hat{q})\right|^2 G(\hat{m}-\hat{p})G(-\hat{m}+\hat{q})\,\mathrm{d}\Omega_p\,\mathrm{d}\Omega_q$$

and

$$A(\boldsymbol{m},\boldsymbol{p},\boldsymbol{q}) = P_{\alpha\beta\gamma}(\boldsymbol{m})P_{\alpha\delta\lambda}(\boldsymbol{m})P_{\delta\sigma\tau}(\boldsymbol{m}-\boldsymbol{q})P_{\gamma\rho\nu}(\boldsymbol{m}-\boldsymbol{p})P_{\tau\nu}(\boldsymbol{m}-\boldsymbol{p}-\boldsymbol{q})P_{\beta\sigma}(\boldsymbol{p})P_{\lambda\rho}(\boldsymbol{q})$$

which leads to

$$J_4(\varepsilon) = \int_\varepsilon^\infty \int_\varepsilon^\infty \frac{y(1+x)(2+y)(3+x+y)-(2+x)(2+x+y)(1+3y+y^2)}{x^2y^2(1+x)(2+x)(1+y)^2(2+y)(1+x+y)}\,\mathrm{d}x\,\mathrm{d}y. \tag{127}$$

Evaluation of the four integrals yields the divergent terms

$$J_1(\varepsilon) = \left(\frac{47}{6}-\frac{1}{4}\log 2\right)\log\varepsilon + \frac{25}{4}\log^2\varepsilon + \frac{3}{\varepsilon}+\frac{2}{\varepsilon^2}+\frac{13}{2}\frac{\log\varepsilon}{\varepsilon} \tag{128}$$

$$\begin{aligned} J_2(\varepsilon) &= -\left(\frac{5}{2}-\frac{1}{4}\log 2\right)\log\varepsilon - \frac{9}{4}\log^2\varepsilon - \frac{1}{2}\frac{1}{\varepsilon} - \frac{1}{\varepsilon^2} - \frac{5}{2}\frac{\log\varepsilon}{\varepsilon} \\ J_3(\varepsilon) &= \left(9+\frac{1}{2}\log 2\right)\log\varepsilon + \frac{15}{2}\log^2\varepsilon + \frac{3}{\varepsilon}+\frac{2}{\varepsilon^2}+8\frac{\log\varepsilon}{\varepsilon} \end{aligned} \tag{129}$$

and

$$J_4(\varepsilon) = -\left(2+\frac{1}{2}\log 2\right)\log\varepsilon - \frac{5}{2}\log^2\varepsilon - \frac{1}{\varepsilon} - \frac{1}{\varepsilon^2} - 4\frac{\log\varepsilon}{\varepsilon}. \tag{130}$$

The sum of the divergences is thus

$$\sum_{s=1}^{4} J_s(\varepsilon) = \frac{37}{3}\log\varepsilon + 9\log^2\varepsilon + \frac{9}{2}\frac{1}{\varepsilon} + \frac{2}{\varepsilon^2} + 8\frac{\log\varepsilon}{\varepsilon} \tag{131}$$

which is identical to the sum of the divergences obtained in (115) for $\Gamma_2(\hat{m})$.

It now follows from (75), (103), (108), (115), (117), (125) and (131) that the ratios of the divergences of the 2-loop terms to the tree level terms for the two 1PI functions, from which Z_D and Z_ν are calculated, are equal, as we found at 1-loop order, specifically

$$\sum_{s=1}^{2} \frac{\Gamma_2^{(s)}(\hat{m})}{\Gamma_0(\hat{m})} = \sum_{s=1}^{4} \frac{\Pi_2^{(s)}(\hat{m})}{\Pi_0(\hat{m})}.$$

Thus, like the 1-loop terms (122), the 2-loop terms also have identical divergences. So the coefficient a_{2D} in (116) must equal the corresponding coefficient $a_{2\nu}$ in (69). In fact, using the 2-loop counterterm

$$a_{2D} g^2 D(\mu) \log\left(\frac{\mu}{\kappa}\right)$$

to eliminate the logarithmic divergences of $\Pi_2(\hat{m})$ as given by (125) and (131) yields

$$a_{2D} = -\tfrac{37}{2}$$

as in the case of $a_{2\nu}$.

The fact that the renormalization constants Z_D and Z_ν are equal is a dynamical condition which indicates that the Kolmogorov scaling of the equal time correlators is preserved under this renormalization. This happens because D and ν are intervening nonlinear variables, representing the basic cascade mechanism and relating to a constant mean dissipation rate, as already indicated and further elaborated in section 8. It implies that the usual perturbative mechanisms do not modify the Kolmogorov scaling, so that one is led to look elsewhere for an explanation of multiscaling. The same conclusion has been reached, albeit from a somewhat different perspective, in [15] where it has been suggested that corrections to Kolmogorov scaling should be sought in non-perturbative effects, such as resummation of ladder diagrams [16]. Our argument is that the breaking of the Kolmogorov scale symmetry manifests itself through the composite operators which appear in the structure functions, as described in section 3, and that the anomalies can be found directly from the nonlinear Green functions to be introduced in the next section. Of course, if our calculation had been based on the viscous zero-order quadratic form in (21), instead of the modified form in (26), then this relation would not hold.

4.3. The fixed point

The equality of Z_ν and Z_D allows us to calculate the uv fixed point from the linear response function alone as follows. We use the standard result [14]

$$\beta(g) = -g\,\mu \frac{\partial}{\partial \mu} \log Z_g \left(1 + g\,\frac{\partial}{\partial g} \log Z_g\right)^{-1} \tag{132}$$

where Z_g is the renormalization constant associated with the coupling constant. From the definition $Z_g = g_0/g$ and (32), (35), (36) and (43), we get

$$Z_g = Z_\nu^{-2}.$$

Inserting this result in (132), and substituting the expansion (69), leads to

$$\beta\,(g) = 2g^2(1 + a_{2\nu} g). \tag{133}$$

Thus, (67), (68), (114) and (133) yield an uv fixed point given by

$$g_* = -\frac{1}{a_{2\nu}} = \frac{2}{37}. \tag{134}$$

We see that g_* is, indeed, small, which verifies that the residual coupling associated with the fluctuation of the dissipation can be treated as weak.

5. The nonlinear response

Having established that an uv fixed point exists, we can proceed with the calculation of the anomalous dimension γ_s of the general operator $O_s(\hat{x})$, which is required for the evaluation of the anomaly τ_n. To do this in the simplest possible way, we must identify a 1PI response function which can be renormalized by means of Z_s. Elimination of the logarithmic divergences from such a function will then enable us to determine the constants in the expansion

$$Z_s = 1 + g_* a_1^{(s)} \log\left(\frac{\mu}{\kappa}\right) + g_*^2 \left\{ \frac{1}{2}\left(a_1^{(s)}\right)^2 \log^2\left(\frac{\mu}{\kappa}\right) + a_2^{(s)} \log\left(\frac{\mu}{\kappa}\right) \right\} + \cdots \tag{135}$$

so that we can calculate γ_s using (49).

Consider first the case $s = 2$. Obviously, the required function must involve $O_2(\hat{x})$, which is the composite operator (31) associated with the longitudinal turbulence energy. In addition, it must involve the dynamic response operator (11) in order to relate the anomaly τ_2 to the dynamics of the turbulence. This suggests that we should consider how the turbulence energy responds on average to a change in the forcing. Clearly, we can characterize the response of the turbulence energy at a point $\hat{x}$ to a change in the forcing at two points $\hat{x}'$ and $\hat{x}''$ by means of the nonlinear Green function

$$G^{(2)}_{\alpha\beta}(\hat{x}', \hat{x}'', \hat{x}) = \left\langle \frac{\delta^2}{\delta f_\alpha(\hat{x}')\delta f_\beta(\hat{x}'')} \left(\frac{v_1(\hat{x})^2}{2} \right) \right\rangle. \tag{136}$$

But the complexity of this object is such that its logarithmic divergences cannot be summed using the renormalization group in terms of the Z_2 and Z_ν counterterms alone. On the other hand, its average $\overline{G}^{(2)}_{\alpha\beta}(\hat{x})$ taken over the forcing separation $\hat{x}' - \hat{x}''$, which gives a mean response to forcing at the centroid of the excitation points, can be, as we shall show shortly. Hence, its corresponding 1PI function provides a direct means of obtaining the expansion (135) and so it provides an adequate basis for the calculation of γ_2.

This 1PI function is obtained as follows. We start with the Fourier transform of (136), the reduced form of which is given by

$$G^{(2)}_{\alpha\beta}(\hat{k}, \hat{l}, \hat{p}) = (2\pi)^4 \delta(\hat{k} + \hat{l} + \hat{p}) G^{(2)}_{\alpha\beta}(\hat{k}, \hat{l}) \tag{137}$$

where

$$G^{(2)}_{\alpha\beta}(\hat{k}, \hat{l}) = P_{\alpha 1}(\boldsymbol{k})\, P_{\beta 1}(\boldsymbol{l})\, G_2(\hat{k}, \hat{l}). \tag{138}$$

Its corresponding 1PI response function follows from

$$\Theta^{(2)}_{\alpha\beta}(\hat{k}, \hat{l}, \hat{p}) = (2\pi)^{12} \frac{\delta^3 K}{\delta u_\alpha(\hat{k})\delta u_\beta(\hat{l})\delta t_2(-\hat{p})} \tag{139}$$

with a reduced form given by

$$\Theta^{(2)}_{\alpha\beta}(\hat{k}, \hat{l}, \hat{p}) = (2\pi)^4 \delta(\hat{k} + \hat{l} + \hat{p}) \Theta^{(2)}_{\alpha\beta}(\hat{k}, \hat{l}) \tag{140}$$

where

$$\Theta^{(2)}_{\alpha\beta}(\hat{k}, \hat{l}) = P_{\alpha 1}(\boldsymbol{k}) P_{\beta 1}(\boldsymbol{l}) \Theta^{(2)}(\hat{k}, \hat{l}). \tag{141}$$

A standard calculation [7] shows that it is related to $G^{(2)}_{\alpha\beta}$ by

$$\Theta^{(2)}_{\alpha\beta}(\hat{k}, \hat{l}, \hat{p}) = -\int \Gamma_{\lambda\alpha}(\hat{q}, \hat{k})\, \Gamma_{\mu\beta}(\hat{q}', \hat{l})\, G^{(2)}_{\lambda\mu}(\hat{q}, \hat{q}', \hat{p})\, \mathrm{d}\hat{q}\, \mathrm{d}\hat{q}' \tag{142}$$

from which, on making use of (137)–(141), we obtain

$$\Theta^{(2)}(\hat{k}, \hat{l}) = -\Gamma(\hat{k})\Gamma(\hat{l}) G_2(\hat{k}, \hat{l}). \tag{143}$$

Next, we average $G^{(2)}_{\alpha\beta}$ over the forcing separation to get

$$\overline{G}_{\alpha\beta}(\hat{x}) = 2\int G^{(2)}_{\alpha\beta}(\hat{k},\hat{k})\exp(2\mathrm{i}\hat{k}\cdot\hat{x})\,\mathrm{D}\hat{k}. \tag{144}$$

This integral shows that the Fourier transform of $\overline{G}^{(2)}_{\alpha\beta}(\hat{x})$ depends only on the diagonal components of the reduced function (138). It follows, therefore, from (143) and (144), that the 1PI object which we need to consider, in order to determine Z_2, is

$$\Theta^{(2)}(\hat{k},\hat{k}) = -\Gamma(\hat{k})^2 G_2(\hat{k},\hat{k}).$$

Indeed, an application of (37), together with (73), shows that its bare and renormalized forms are connected by

$$\Theta^{(2)}_{\mathrm{R}}(\hat{k},\hat{k}) = Z_2\Theta^{(2)}_{\mathrm{B}}(\hat{k},\hat{k}).$$

In this way, as we have indicated, we arrive at a function which can be renormalized using the Z_2 counterterm alone.

The normalization condition for $\Theta^{(2)}(\hat{k},\hat{k})$ is again applied at the point $\hat{k}=\hat{m}$, and chosen to be consistent with the tree level approximation in conformity with (135), which gives

$$\Theta^{(2)}(\hat{m},\hat{m}) = \Theta^{(2)}_0(\hat{m},\hat{m}) = -1 \tag{145}$$

so that the 1- and 2-loop terms satisfy the normalization conditions

$$\Theta^{(2)}_1(\hat{m},\hat{m}) = \Theta^{(2)}_2(\hat{m},\hat{m}) = 0. \tag{146}$$

The diagrams which yield the new logarithmic divergences to 2-loop order, which are associated with the composite operator, are shown in figure 5 for the case of $\Theta^{(2)}_{\alpha\beta}(\hat{m},\hat{m})$, which is related to $\Theta^{(2)}(\hat{m},\hat{m})$ by (141). An important new feature of these diagrams is the appearance of the heavy dot vertex. This represents the O_2 composite operator vertex, which is shown in figure 1(iv) for the general case of O_{s}. A second difference from earlier diagrams is that each external leg carrying one of the vector indices (α, say) has a projector $P_{\alpha\lambda}(\boldsymbol{m})$ associated with it, which is contracted with the vector index λ of the leg of the NS vertex to which it is attached, in accordance with (142).

We can understand how the diagrams shown in figure 5 arise from the loop expansion of K by using the general procedure described in [17]. This depends on the fact that (136) is a special case of the fourth-order correlation function of elementary fields defined by

$$B^{(4)}_{\alpha\beta\gamma\delta}(\hat{x}',\hat{x}'',\hat{x},\hat{z}) = \frac{\mathrm{i}^2}{2}\left\langle\tilde{v}_\alpha(\hat{x}')\tilde{v}_\beta(\hat{x}'')v_\gamma(\hat{x})v_\delta(\hat{z})\right\rangle$$

in which the arguments $\hat{x}$ and $\hat{z}$ coalesce. Hence, their Fourier transforms are related. In particular, the connection between their respective 1PI functions is

$$\Theta^{(2)}_{\alpha\beta}(\hat{k},\hat{l},\hat{m}) = \tfrac{1}{2}\int\Phi_{\alpha\beta\lambda\mu}(\hat{k},\hat{l},\hat{m}-\hat{q},\hat{q})G_{\lambda 1}(\hat{m}-\hat{q})G_{\mu 1}(\hat{q})\,\mathrm{D}\hat{q}$$

where Φ is the 1PI form corresponding to $B^{(4)}$, which is generated by

$$\Phi_{\alpha\beta\gamma\delta}(\hat{k},\hat{l},\hat{p},\hat{q}) = (2\pi)^{16}\frac{\delta^4 K}{\delta u_\alpha(\hat{k})\delta u_\beta(\hat{l})\mathrm{i}\delta\tilde{u}_\gamma(\hat{p})\mathrm{i}\delta\tilde{u}_\delta(\hat{q})}.$$

This implies that the diagrams for $\Theta^{(2)}_{\alpha\beta}(\hat{m},\hat{m})$ are constructed from the diagrams for Φ by tying the two dotted external legs of the latter to form the O_2 vertex.

The 1-loop diagram for $\Theta^{(2)}_{\alpha\beta}(\hat{m},\hat{m})$ shown in figure 5(iv) is constructed from the tree level diagram for Φ, which is shown opposite to it in figure 5(i). Similarly, the two 2-loop diagrams for $\Theta^{(2)}_{\alpha\beta}(\hat{m},\hat{m})$, shown in figures 5(v) and (vi), are constructed from the 1-loop diagrams for Φ,

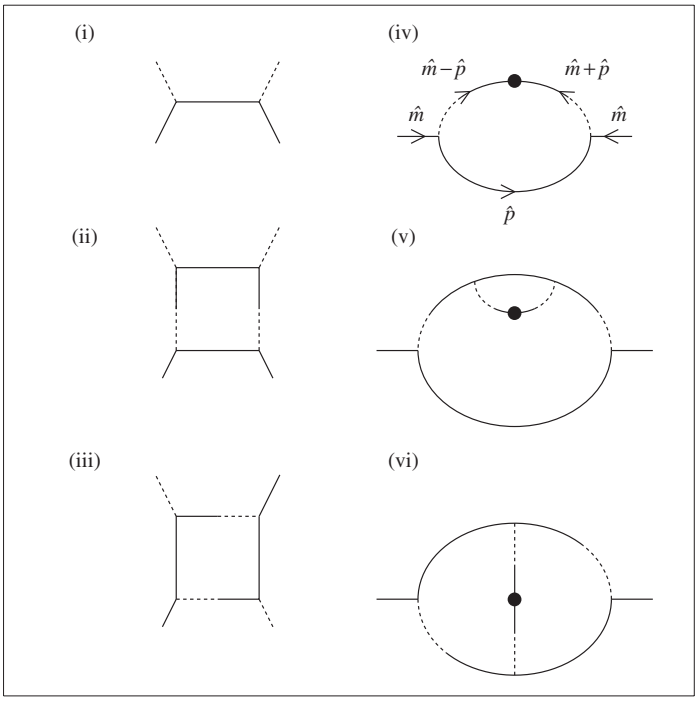

Figure 5. The 1PI Feynman diagrams evaluated in section 5 for the nonlinear response functions.

again shown opposite to them in figures 5(ii) and (iii). The other possible 2-loop diagrams for $\Theta^{(2)}_{\alpha\beta}(\hat{m},\hat{m})$, which arise from the two remaining 1-loop diagrams for Φ, are discarded because the logarithmic divergences disappear, after integration over the solid angles. In addition, vertex and propagator corrections to the tree level diagram 5(i) make no contribution to the new divergences associated with the composite operator, as discussed further below.

Thus, the 1-loop diagram of figure 5(iv) contributes to $\Theta^{(2)}_1$ the term

$$P_{\alpha 1}(\boldsymbol{m})P_{\beta 1}(\boldsymbol{m})\Theta^{(2)\prime}_1(\hat{m},\hat{m}) = \int \mathrm{D}\boldsymbol{p}\,\mathrm{D}\Omega\, G_{\lambda 1}(-\hat{m}+\hat{p})G_{\nu 1}(-\hat{m}-\hat{p})Q_{\gamma\delta}(\hat{p}) \times P_{\lambda\gamma\alpha}(\boldsymbol{m}-\boldsymbol{p})P_{\nu\delta\beta}(\boldsymbol{m}+\boldsymbol{p})P_{\alpha\lambda}(\boldsymbol{m})P_{\beta\mu}(\boldsymbol{m}) \tag{147}$$

yielding

$$\Theta^{(2)\prime}_1(\hat{m},\hat{m}) = \tfrac{3}{2}gI_0(\varepsilon)$$

where I_0 is the integral (89). Using (79) and (88) we get a logarithmic divergence

$$\Theta^{(2)\prime}_1(\hat{m},\hat{m}) = -g\log\left(\frac{\mu}{\kappa}\right). \tag{148}$$

The counterterm vertex shown in figure 2(iii) adds a term

$$-P_{\alpha 1}(\boldsymbol{m})P_{\beta 1}(\boldsymbol{m})\Theta^{(2)\prime\prime}_1(\hat{m},\hat{m}) = -P_{\alpha 1}(\boldsymbol{m})\,P_{\beta 1}(\boldsymbol{m})\,\Delta Z_2$$

so that by (135) its contribution to $\Theta^{(2)}_1$ is

$$\Theta^{(2)\prime\prime}_1(\hat{m},\hat{m}) = -a^{(2)}_1 g\log\left(\frac{\mu}{\kappa}\right). \tag{149}$$

But, from the normalization condition (146), we have

$$\Theta^{(2)}_1(\hat{m},\hat{m}) = \Theta^{(2)\prime}_1(\hat{m},\hat{m}) + \Theta^{(2)\prime\prime}_1(\hat{m},\hat{m}) = 0$$

which, upon substituting (148) and (149), gives

$$a_1^{(2)} = -1. \tag{150}$$

At 2-loop order the diagrams in figures 5(v) and (vi) contribute the terms

$$\begin{aligned} P_{\alpha 1}(\boldsymbol{m})P_{\beta 1}(\boldsymbol{m})\Theta_2^{(2)\prime}(\hat{m},\hat{m}) = -\int \mathrm{D}\hat{p}\,\mathrm{D}\hat{q}\; & Q_{\gamma\delta}(\hat{p})Q_{\rho\tau}(\hat{q})G_{\theta\nu}(-\hat{m}+\hat{p})G_{\sigma\phi}(-\hat{m}-\hat{p}) \\ & \times G_{\epsilon 1}(-\hat{m}+\hat{p}+\hat{q})G_{\kappa 1}(-\hat{m}-\hat{p}-\hat{q})P_{\alpha\lambda}(\boldsymbol{m})P_{\beta\mu}(\boldsymbol{m}) \\ & \times P_{\theta\lambda\gamma}(\boldsymbol{m}-\boldsymbol{p})P_{\phi\mu\delta}(\boldsymbol{m}+\boldsymbol{p})P_{\epsilon\nu\rho}(\boldsymbol{m}-\boldsymbol{p}-\boldsymbol{q})P_{\kappa\tau\sigma}(\boldsymbol{m}+\boldsymbol{p}+\boldsymbol{q}) \end{aligned}$$

and

$$\begin{aligned} P_{\alpha 1}(\boldsymbol{m})P_{\beta 1}(\boldsymbol{m})\Theta_2^{(2)\prime\prime}(\hat{m},\hat{m}) = -\int \mathrm{D}\hat{p}\,\mathrm{D}\hat{q}\; & Q_{\gamma\nu}(\hat{p})Q_{\delta\tau}(\hat{q})G_{\theta\rho}(-\hat{m}+\hat{p})G_{\sigma\phi}(-\hat{m}+\hat{q}) \\ & \times G_{\epsilon 1}(-\hat{m}+\hat{p}-\hat{q})G_{\kappa 1}(-\hat{m}-\hat{p}+\hat{q})P_{\alpha\lambda}(\boldsymbol{m})P_{\beta\mu}(\boldsymbol{m}) \\ & \times P_{\theta\lambda\gamma}(\boldsymbol{m}-\boldsymbol{p})P_{\phi\mu\delta}(\boldsymbol{m}+\boldsymbol{p})P_{\epsilon\rho\tau}(\boldsymbol{m}-\boldsymbol{p}+\boldsymbol{q})P_{\kappa\nu\sigma}(\boldsymbol{m}+\boldsymbol{p}-\boldsymbol{q}). \end{aligned}$$

Evaluating these integrals following the procedure described in section 4, we get

$$\Theta_2^{(2)\prime}(\hat{m},\hat{m}) = -\tfrac{9}{4}g^2 J_3(\varepsilon)$$

and

$$\Theta_2^{(2)\prime\prime}(\hat{m},\hat{m}) = \tfrac{9}{4}g^2 J_4(\varepsilon)$$

where J_3 and J_4 are the integrals (126) and (127). Using (129) and (130), we obtain the logarithmic divergences

$$\Theta_2^{(2)\prime}(\hat{m},\hat{m}) = \frac{9}{4}g^2\left(\frac{5}{3}-\frac{1}{6}\log 2\right)\log\left(\frac{\mu}{\kappa}\right) \tag{151}$$

and

$$\Theta_2^{(2)\prime\prime}(\hat{m},\hat{m}) = \frac{9}{4}g^2\left(\frac{4}{3}+\frac{1}{3}\log 2\right)\log\left(\frac{\mu}{\kappa}\right). \tag{152}$$

To these we must add the 2-loop counterterm corresponding to (149), namely

$$\Theta_2^{(2)\prime\prime\prime}(\hat{m},\hat{m}) = -a_2^{(2)}g^2\log\left(\frac{\mu}{\kappa}\right). \tag{153}$$

But the normalization condition (146) gives

$$\Theta_1^{(2)\prime}(\hat{m},\hat{m}) + \Theta_1^{(2)\prime\prime}(\hat{m},\hat{m}) + \Theta_1^{(2)\prime\prime\prime}(\hat{m},\hat{m}) = 0$$

which, after substituting (151)–(153), yields

$$a_2^{(2)} = 7.0. \tag{154}$$

If vertex and propagator corrections are allowed for (which only affects diagram 5(iv) to order g^2), it is found that the pole at $\Omega = \mathrm{i}\sigma(\mu)$ in the integral (147), which generates its logarithmic divergence, is shifted by an amount

$$\Delta\Omega = -\sigma(\mu)\Gamma_1'(\hat{m})$$

where

$$\Gamma_1'(\hat{m}) = \left(\frac{\partial\Gamma_1(\hat{p})}{\partial\Omega}\right)_{\hat{p}=\hat{m}}$$

thereby introducing into the integrand an additional factor

$$1-\Gamma_1'(\hat{m}). \tag{155}$$

However, this is exactly cancelled by the NS vertex correction. For, from the Ward identity associated with the Galilean invariance [18], it follows that the change in the NS vertex at the normalization point is given by

$$\Delta P_{\alpha\beta\gamma}(\boldsymbol{m}) = \mathrm{i}m_\gamma P_{\alpha\beta}(\boldsymbol{m})\Gamma_1'(\hat{m}) \tag{156}$$

so that the angular factor in (147) becomes

$$P_{\alpha 1}(\boldsymbol{m})P_{\beta 1}(\boldsymbol{m})\{1+\Gamma_1'(\hat{m})\}. \tag{157}$$

Thus, no overall term of order g^2 is produced by the two corrections (155) and (157). It may be noted, in passing, that the Ward identity (156) can be derived by functional differentiation of the condition (165) for the invariance of W with respect to an infinitesimal Galilean transformation given later in section 7.

The foregoing can be generalised to arbitrary s. In place of (139), we now consider the general 1PI response function

$$\Theta^{(s)}_{\alpha_1\ldots\alpha_s}(\hat{k}_1,\ldots,\hat{k}_s,\hat{p}) = (2\pi)^{4(s+1)}\frac{\delta^{s+1}K}{\delta u_{\alpha_1}(\hat{k}_1)\ldots\delta u_{\alpha_s}(\hat{k}_s)\delta t_s(-\hat{p})}$$

with a reduced form defined by

$$\Theta^{(s)}_{\alpha_1\ldots\alpha_s}(\hat{k}_1,\ldots,\hat{k}_s,\hat{p}) = (2\pi)^4\delta(\hat{k}_1+\cdots+\hat{k}_s+\hat{p})P_{\alpha_1 1}(\boldsymbol{k}_1)\ldots P_{\alpha_s 1}(\boldsymbol{k}_s)\Theta^{(s)}(\hat{k}_1,\ldots,\hat{k}_s).$$

Then Z_s can be found by eliminating the logarithmic divergences from the diagonal component $\Theta^{(s)}(\hat{m},\ldots,\hat{m})$ as above. The relevant diagrams are again those shown in figures 5(iv)–(vi), except that the heavy dot now symbolises the O_s vertex of figure 1(iv), so the $s-2$ external legs of O_s are not shown explicitly. Each diagram has a symmetry factor $s(s-1)/2$. As this is the only respect in which these diagrams differ from those just considered, we have the relation

$$a^{(s)}_{1,2} = \frac{s(s-1)}{2}a^{(2)}_{1,2}. \tag{158}$$

However, this is an approximate result, because it is not valid for diagrams containing more than 2-loops. But, as we discuss further below, it suffices for the calculation of low-order exponents. Thus, we have now calculated all the numerical constants that we require for the evaluation of ζ_n.

6. The scaling exponents

For $n=2$, we have, from (53),

$$\zeta_2 = \tfrac{2}{3} + \Delta_2$$

where, from (49), (54) and (135).

$$\Delta_2 = -g_*(a_1^{(2)} + a_2^{(2)}g_*). \tag{159}$$

Substituting the numerical values calculated above, as given in (134), (150) and (154), we get

$$\Delta_2 = \tfrac{46}{37^2} = 0.0336$$

which yields

$$\zeta_2 = 0.70.$$

For $n=3$, we shall verify in section 8 that the known exact result

$$\zeta_3 = 1$$

holds.

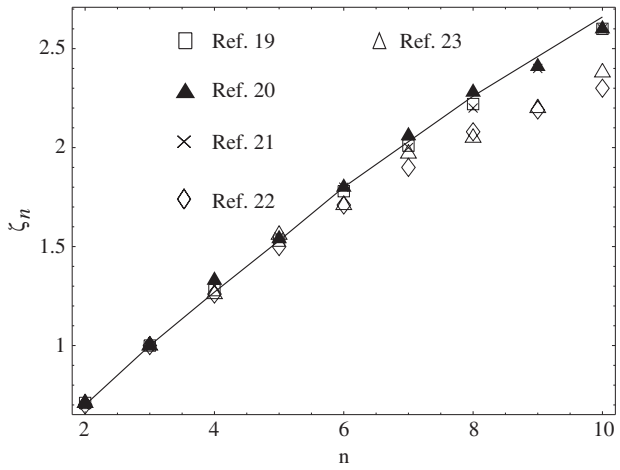

Figure 6. Comparison of the theoretical expression for ζ_n (full line) with experimental data.

In the general case, for $n > 3$, we have from (64)

$$\zeta_n = \frac{n}{3} - \tau_n.$$

For even orders $n = 2m$, the anomaly is given by (65),

$$\tau_n = \max_p \tau_{np}. \tag{160}$$

But, from (49), (63), (135), (158) and (159), we have

$$\tau_{np} = \{p(p-1) + (n-p)(n-p-1) - 2(m-p)[2(m-p)-1]\}\,\frac{\Delta_2}{2}.$$

A simple calculation shows that the maximum value of this expression is attained by the two terms in the series (58) with (a) $p = m$ and (b) $p = m - 1$; which gives for (160)

$$\tau_n = m(m-1)\Delta_2. \tag{161}$$

For odd orders, $n = 2m + 1$, the anomaly is given directly by (66), which yields

$$\tau_n = m^2\Delta_2$$

where we have again used (49), (135), (158) and (159).

The above results have been used to calculate ζ_n up to $n = 10$. The results are shown in figure 6, together with the experimental data taken from [19–23]. It can be seen that the agreement is good up to about $n = 7$ and fair beyond, if we allow for the uncertainties in the experimental data which begin to arise. In particular, it may be noted that the key values $\zeta_2 = 0.70$ and $\zeta_6 = 1.8$ are in good agreement with experimental data, the respective data sets from [19–23] giving for ζ_2 the values (0.71, 0.70, 0.71, 0.70, 0.71) and for ζ_6 the values (1.78, 1.8, 1.8, 1.71, 1.71). The divergence of the experimental data at higher orders reflects the fact that the experimental determination of ζ_n is not yet fully satisfactory for the reasons given in [23]. Hence, the good agreement between our calculations at higher values of n with the particular data sets from [19–21] must be treated with caution, particularly as the expression we have derived above is not applicable at large orders. This limitation stems from the fact that the mean nonlinear response function, being an average over the forcing configuration, does not represent the effect of multiple correlations with sufficient accuracy at large n. In addition, the approximation (158), as we have noted, only holds up to 2-loop order. Indeed, it

is evident from the foregoing that the overall approximation must fail when $ng_* \sim 1$. However, this occurs at roughly $n = 20$, which is well above the current limit of reliable experimental data. Equally, the divergence of our theoretical values at higher values of n from the other two data sets [22, 23] could indicate that the accuracy of our low order approximation is already beginning to deteriorate at around $n \sim 10$.

7. Elimination of sweeping

We now return to the question of the power and power $\times$ logarithmic divergences which, up to this point, we have simply discarded on the grounds that they cancel when sweeping convection is taken into account. The fact that power divergences arise when field-theoretic methods are applied to turbulence, using an Eulerian approach, was noticed originally in [24]. Their origin was subsequently identified as being due to the kinematic effect of the sweeping of small eddies by large eddies, having an almost uniform velocity [25, 26]. The remedy was to change from an Eulerian to a Lagrangian description, but this greatly complicates the subsequent analysis [27]. However, it has been shown that the elimination of sweeping can be accomplished more simply by transforming to a frame moving with the local velocity of the large-scale eddies at some chosen reference point, [28, 29]. We shall show that a similar approach can be used to eliminate the power and power $\times$ logarithmic divergences within the present framework. In this way, we shall demonstrate that, although we have started out from an Eulerian formulation, we ultimately obtain quasi-Lagrangian approximations for the renormalized functions.

The problem, therefore, is to find a sweeping interaction term, ΔL_s, which cancels the effect of sweeping convection. To this end, let us begin by including in the NS equations (4) a uniform convection $\boldsymbol{U}$. Then, in the second term of (26), $\boldsymbol{F}(\hat{k}, \boldsymbol{v})$ is replaced by $\boldsymbol{F}(\hat{k}, \boldsymbol{v}) - \mathrm{i}\boldsymbol{k} \cdot \boldsymbol{U}\boldsymbol{v}(\hat{k})$, so that W contains the additional term

$$\exp\left\{\int \boldsymbol{k} \cdot \boldsymbol{U}\, \tilde{\boldsymbol{v}}(-\hat{k}) \cdot \boldsymbol{v}(\hat{k})\, \mathrm{D}\hat{k}\right\}.$$

Let us assume further that $\boldsymbol{U}$ is a random variable having a Gaussian distribution $\propto \exp(-U^2/2U_0^2)$. This permits us to average W over $\boldsymbol{U}$, the result being the addition to L of an interaction term given by

$$\Delta L_U = -\frac{U_0^2}{2} \int \boldsymbol{l} \cdot \boldsymbol{m}\, \tilde{\boldsymbol{v}}(\hat{m}) \cdot \boldsymbol{v}(-\hat{m})\, \tilde{\boldsymbol{v}}(\hat{l}) \cdot \boldsymbol{v}(-\hat{l})\, \mathrm{D}\hat{l}\, \mathrm{D}\hat{m} \tag{162}$$

where, as above, the variables $\boldsymbol{v}$ and $\tilde{\boldsymbol{v}}$ refer to the moving frame. Note that ΔL_U, like L, is Galilean invariant because it entails only gradients of the velocity field.

We show next that a term of this form, with the appropriate value of U_0^2, generates all power divergences arising from the sweeping convection associated with $L(\boldsymbol{v}, \tilde{\boldsymbol{v}})$. Thus, a term of the form (162), with this specific value of U_0^2, but of opposite sign, provides the means to satisfy the condition that convection makes no contribution to the underlying probability distribution in the moving frame, leading, at the fixed point, to a precise form for ΔL_s, as given below in (164). The result is a generating functional which isolates the straining interactions that determine the scaling exponents from the background of sweeping convection.

To represent diagrammatically the additional terms which arise in the loop expansion of W, after the inclusion of the sweeping interaction term, we need to introduce a new 4-leg 'sweeping' vertex of the type shown in figure 7(i). The two wavevectors $\hat{l}$ and $\hat{m}$ in (162) enter this vertex along its continuous legs and leave along the dotted legs. A pair of legs carrying a particular wavevector must also carry the same vector index to represent the scalar

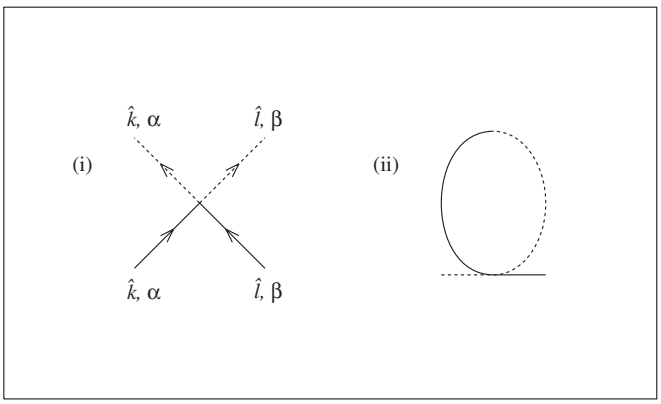

Figure 7. (i) The 'sweeping' vertex; (ii) the 1-loop 'sweeping' Feynman diagram for the linear response function evaluated in section 7.

product. Free wavevectors in a diagram containing one or more of these sweeping vertices are identified, as previously, by overall wavenumber conservation, together with conservation at any NS vertex. Each sweeping vertex then contributes a factor $U_0^2\, \boldsymbol{l} \cdot \boldsymbol{m}$, where $\boldsymbol{l}$ and $\boldsymbol{m}$ are the two wavevectors which enter the vertex along its two continuous legs. In all other respects the diagrams are to be interpreted in accordance with the rules given in section 4.

Consider now the set of diagrams, containing only NS vertices, which are associated with a particular Green function or velocity correlator, $\mathcal{G}$, say. Let C_{NS} denote any such diagram contributing to $\mathcal{G}$. We shall show that it is possible to generate all power and power $\times$ logarithmic divergences of any C_{NS} from a single sweeping interaction of the form (162). Let C_U denote any diagram containing at least one sweeping vertex. If C_U contains no NS vertices at all, then it will only generate power divergences. But if it contains at least one NS vertex, it will also generate power $\times$ logarithmic divergences. The following topological argument demonstrates that the power divergences of C_{NS} can be put into 1–1 correspondence with the C_U diagrams relating to $\mathcal{G}$.

Each factor $\tau(\kappa)$ (or, equivalently, ε^{-1}) in a power divergence of C_{NS} arises because it is possible for a soft wavevector $\boldsymbol{q}$ to flow through a particular velocity correlator without flowing through the active legs of the two NS vertices which it connects, as already discussed in section 4. This situation can be represented diagrammatically by contracting the correlator into a 4-leg vertex formed by merging the two NS vertices which it links, whilst leaving the hard lines in tact. This can be demonstrated as follows. First, the new vertex must consist of two in-coming full lines which carry hard wavevectors, $\boldsymbol{l}$ and $\boldsymbol{m}$ (say), and two outgoing dotted lines along which they leave. This is because two full legs disappear from the merged NS vertices and wavevectors leave NS vertices along the dotted leg. Furthermore, after integrating over the directions of the soft wavevector $\boldsymbol{q}$, the two merged NS vertices generate, through contraction of the projectors, a factor proportional to the scalar product of the in-coming hard lines, $\boldsymbol{l} \cdot \boldsymbol{m}$, while the two legs of a pair carrying the same wavevector acquire the same vector index. The final integration over the wavenumbers then produces the constant

$$\frac{1}{6\pi^2} \int_{\kappa}^{\infty} q^2 D(q) \tau(q)\, \mathrm{d}q = \frac{3}{2} g \tau(\kappa) \nu^3.$$

So, such a vertex must, in fact, be of the sweeping convection type (162), with a coefficient given by

$$U_0^2 = \tfrac{3}{2} g \tau(\kappa) \nu^3 \tag{163}$$

which relates the rms value of the convection velocity to the strength of the nonlinear interaction. Note that U_0 is scale dependent, as it depends on the renormalization scale μ through g and ν, and, hence, it differs according to the fluctuation scale on which the RG focuses. In physical terms, this reflects the fact that the rms convection velocity depends on the scale selected. Changing the renormalization scale does not, of course, affect the Galilean invariance. When the fixed point is reached, in the limit $\mu \to \infty$, corresponding to scale invariance, U_0 has the specific value which is obtained by substituting the fixed point values in (163). In general, as discussed below, the application of an arbitrary infinitesimal Galilean transformation leads to the turbulence Ward identities.

Clearly, if a subset of correlators of $C_{\rm NS}$, each of which carries a soft wavenumber, is contracted into such 4-leg vertices, in a manner which allows hard wavevectors to flow through $C_{\rm NS}$, then the result is a diagram which is identical to one of the C_U diagrams. Moreover, it is clear that there are always exactly as many ways to contract the correlators in $C_{\rm NS}$ as there are different C_U diagrams and that their symmetry factors must match. This argument demonstrates, therefore, the important point that the power and power $\times$ logarithmic divergences generated by the NS vertex must arise on account of the background of kinematic sweeping effects. Moreover, we also see that, in order to cancel them, it is only necessary to introduce a sweeping interaction term into W of opposite sign to the one from which they can be generated, which, according to (162) and (163) yields the sweeping interaction term

$$\Delta L_{\rm s} = \frac{3}{4}\frac{g\nu^3}{\tau(\kappa)} \int \boldsymbol{l}\cdot\boldsymbol{m}\, \tilde{\boldsymbol{v}}(\hat{m})\cdot\boldsymbol{v}(-\hat{m})\, \tilde{\boldsymbol{v}}(\hat{l})\cdot\boldsymbol{v}(-\hat{l})\, \mathrm{D}\hat{l}\, \mathrm{D}\hat{m}. \tag{164}$$

The insertion of $\Delta L_{\rm s}$ into W corresponds, then, to working in a frame moving with the local velocity of the large scale eddies, as given by (163), with $\Delta L_{\rm s}$ cancelling all the contributions of L to the probability that are associated with sweeping convection. Thus, the sweeping vertex shown in figure 7(i) is taken to represent the algebraic factor

$$\text{Vertex 7(i)} = -\tfrac{3}{2} g\tau(k)\nu^3\, \boldsymbol{l}\cdot\boldsymbol{m}.$$

Having inserted (164) into W one is then left with only the pure logarithmic divergences generated by the NS vertex, which, as we have shown, can be summed using the RG.

Given that L, $\Delta L_{\rm s}$ and $O_{\rm s}$, and the measure of integration in W are invariant under a Galilean transformation, the only variation to W under the transformation comes from the source term. In particular, following standard symmetry arguments [7], the requirement for invariance under an infinitesimal transformation $\boldsymbol{v} \to \boldsymbol{v} + \delta\boldsymbol{V}$ and $\boldsymbol{x} \to \boldsymbol{x} - \delta\boldsymbol{V}t$ provides the generating equation for the turbulence Ward identities, as derived in [18], namely

$$\frac{\delta W}{\delta V_\alpha} = \int \mathrm{d}\hat{x} \left\{ -t\tilde{J}_\beta(\hat{x}) \frac{\partial}{\partial x_\alpha} \frac{\delta}{\delta \tilde{J}_\beta(\hat{x})} + J_\alpha(\hat{x}) \right\} W = 0 \tag{165}$$

from which relations such as (156) can be derived by functional differentiation with respect to the source fields $\boldsymbol{J}$ and $\tilde{\boldsymbol{J}}$.

We now illustrate the foregoing by verifying to 2-loop order that $\Gamma(\hat{k})$ contains no power divergences when the contributions from both the NS and the sweeping vertices are included. In section 4, we derived the power divergences that are generated by the NS vertex in the case of $\Gamma(\hat{k})$. At 1-loop order they arise from diagram 3(i), for which (88) and (90) yield, at the normalization point,

$$\Gamma_1 \text{ (diagram 3(i))} = \frac{3}{2} g \frac{\tau(\kappa)}{\tau(\mu)^2}. \tag{166}$$

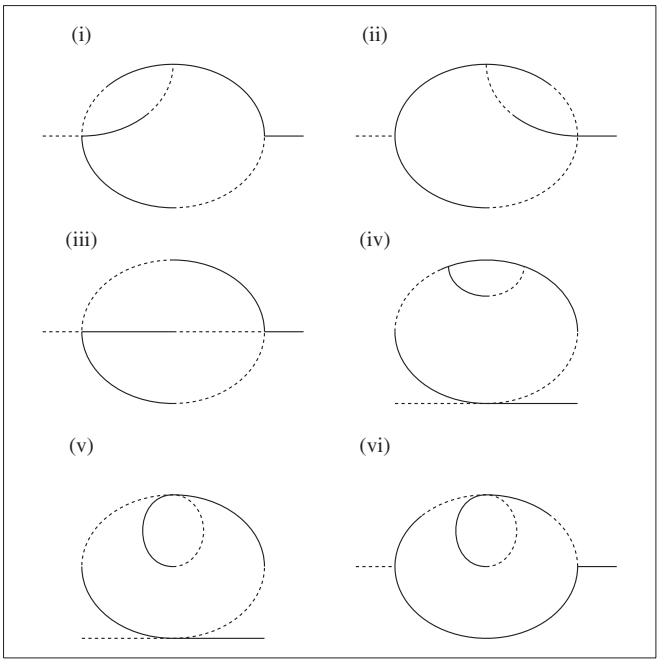

Figure 8. The 2-loop 'sweeping' Feynman diagrams for the linear response function evaluated in section 7.

At 2-loop order they arise from diagrams 3(iii) and (iv). In the first case, (103), (105) and (106) yield

$$\Gamma_2 \text{ (diagram 3(iii))} = -\frac{9}{4}\frac{g^2}{\tau(\mu)}\left\{\frac{1}{\varepsilon^2}+\frac{5}{2}\frac{1}{\varepsilon}+\frac{4}{\varepsilon}\log\varepsilon\right\} \tag{167}$$

while, in the second case, (108), (110) and (111) give

$$\Gamma_2 \text{ (diagram 3(iv))} = -\frac{9}{4}\frac{g^2}{\tau(\mu)}\left\{\frac{1}{\varepsilon^2}+\frac{2}{\varepsilon}+\frac{4}{\varepsilon}\log\varepsilon\right\}. \tag{168}$$

On the other hand, the sweeping vertex makes the following contributions to $\Gamma(\hat{k})$. At 1-loop order, the Feynman rules applied to the sweeping vertex yield the single diagram of figure 7(ii), as we anticipate from the fact that the NS vertices in figure 3(i) can be merged in only one way. In this case, a trivial calculation yields

$$\Gamma_1 \text{ (diagram 7(ii))} = -\frac{3}{2}g\frac{\tau(\kappa)}{\tau(\mu)^2}$$

which cancels (166), as required.

At 2-loop order, the sweeping diagrams corresponding to diagrams 3(iii) and (iv) are shown in figure 8. Explicit verification that there are no power or power×logarithmic divergences in $\Gamma(\hat{k})$ at 2-loop order is less trivial. Consider first diagram (iv) of figure 3. For this diagram the corresponding sweeping diagrams are diagrams (i)–(iii) of figure 8. This follows from the Feynman rules and can be checked from diagram (iv) of figure 3. by first contracting its correlators individually and then together. By applying the Feynman rules to diagram (i) of figure 8, we obtain, at the normalization point,

$$P_{\alpha\beta}(\boldsymbol{m})\Gamma_2 \text{ (diagram 8(i))} = \tfrac{3}{2}g\tau(\kappa)\nu^3\int \boldsymbol{p}\cdot(\boldsymbol{k}-\boldsymbol{p})P_{\lambda\sigma\nu}(\boldsymbol{m})P_{\tau\rho\beta}(\boldsymbol{m}-\boldsymbol{p})$$

$$\times Q_{\rho\nu}(\hat{p})G_{\alpha\lambda}(\hat{m})G_{\sigma\mu}(\hat{m}-\hat{p})G_{\mu\tau}(\hat{m}-\hat{p})\mathrm{D}\hat{p}.$$

We can evaluate this integral using the method described in section 4. This gives

$$\begin{aligned}\Gamma_2\ (\text{diagram 8(i)}) &= \frac{9}{4}\frac{g^2}{\tau(\mu)}\frac{1}{\varepsilon}\int_\varepsilon^\infty \frac{\mathrm{d}x}{x^2(x+1)^2}\\ &= \frac{9}{4}\frac{g^2}{\tau(\mu)}\left\{\frac{1}{\varepsilon^2}+\frac{2}{\varepsilon}\log\varepsilon+\frac{1}{\varepsilon}\right\}.\end{aligned}$$

Diagram (ii) of figure 8 yields the same value

$$\Gamma_2\ (\text{diagram 8(ii)}) = \Gamma_2\ (\text{diagram 8(i)}).$$

Finally, evaluation of the diagram(iii) of figure 8 is trivial and yields

$$\Gamma_2\ (\text{diagram 8(iii)}) = -\frac{9}{4}\frac{g^2}{\tau(\mu)}\frac{1}{\varepsilon^2}.$$

Evidently, the sum of these three diagrams cancels (168) exactly.

Similarly, we can show that the sweeping vertex eliminates the power divergences arising from the second 2-loop diagram, shown in figure 3(iii). In this case, the corresponding diagrams generated by the sweeping vertex are diagrams (iv), (vi) of figure 8 which contribute the terms

$$\Gamma_2\ (\text{diagram 8(iv)}) = \frac{9}{4}\frac{g^2}{\tau(\mu)}\left\{\frac{1}{\varepsilon^2}+\frac{1}{\varepsilon}\log\varepsilon\right\}$$

$$\Gamma_2\ (\text{diagram 8(v)}) = -\frac{9}{4}\frac{g^2}{\tau(\mu)}\frac{1}{\varepsilon^2}$$

and

$$\Gamma_2\ (\text{diagram 8(vi)}) = \frac{9}{4}\frac{g^2}{\tau(\mu)}\left\{\frac{1}{\varepsilon^2}+\frac{3}{\varepsilon}\log\varepsilon+\frac{5}{2}\frac{1}{\varepsilon}\right\}.$$

Again, their sum exactly cancels (167). We have thereby verified to 2-loop order that the sweeping vertex eliminates power divergences generated by the NS vertex from the linear response function.

8. The Kolmogorov approximation

The fact that it has been possible to calculate the anomalies successfully by means of perturbation theory stems, in part, from the incorporation of the Kolmogorov theory into the zero order approximation. As we have seen, this has been done by replacing the actual viscous quadratic form in W, arising from the NS equations, by a modified quadratic form, characterised by an effective random stirring force spectrum $D(k)$ and the effective timescale $\tau(k)$. We now demonstrate that these two functions can be deduced self-consistently as part of the calculation and confirm that that they do have the inertial range forms given in (28) and (29).

To determine these functions, we need two conditions. As in [10], one condition is supplied by evaluating the energy equation to 1-loop order, which gives the convergent DIA form, corresponding to the so-called line renormalization [27]. In the inertial range, it reduces to the condition that the energy flux across wavenumbers $\Pi_\mathrm{E}(k)$ is independent of k and equal to the mean dissipation rate ϵ:

$$\Pi_\mathrm{E}(k) = \epsilon.$$

Thus, evaluation of $\Pi_{\rm E}(k)$ to 1-loop order gives the well known result [27]

$$\Pi_{\rm E}(k) = \int_k^\infty T(p)\,{\rm d}p$$

where

$$T(p) = 8\pi^2 \int\int_\Delta {\rm d}q\,{\rm d}r\,\frac{p^3 qr}{\tau(p)^{-1}+\tau(q)^{-1}+\tau(r)^{-1}} \times \{b(p,q,r)Q(r)(Q(q)-Q(p)) + b(p,r,q)Q(q)(Q(r)-Q(p))\}. \quad (169)$$

Here Δ indicates integration over the region of the p,q plane in which p,q,r can form a triangle and

$$b(p,q,r) = \frac{\left(p^2+q^2-r^2\right)^3}{8p^4q^2} + \frac{r^4-\left(p^2-q^2\right)^2}{4p^2r^2}.$$

The second condition must be deduced from the linear response function. This is where difficulties have arisen with this approach in the past, when using an Eulerian framework, because of the ir divergences arising from sweeping. On the other hand, it is known that no divergence problems arise from sweeping convection in the case of the energy equation [27]. However, we have just shown how these power divergences can be systematically removed from the response function (and, indeed, all such functions) by means of a random Galilean transformation of the velocity field. This leaves the logarithmic divergences which, as we have seen, are to be eliminated from $\Gamma(\hat{k})$ using the Z_ν counterterm. Recall that to fix the finite part of $\Gamma(\hat{k})$, after this renormalization, we imposed the normalization condition (75) which specifies that its tree level term should be exact at the normalization scale μ. Thus, after eliminating sweeping convection, as described in section 7, and using the 1-loop normalization condition (75) to eliminate the logarithmic divergences, we obtain, at an arbitrary wavevector $\boldsymbol{k}$ (with $\omega = 0$), the renormalized linear response function

$$\Gamma(\boldsymbol{k},0) = \tau(k)^{-1} + \frac{\mu^2\tau(\mu)^3 - k^2\tau(k)^3}{6\pi^2\tau(k)\tau(\mu)} \int_0^\infty \frac{p^2\tau(p)^2 D(p)\,{\rm d}p}{(\tau(k)+\tau(p))\,(\tau(\mu)+\tau(p))} + \frac{\mu^2\tau(\mu)^2 - k^2\tau(k)^2}{6\pi^2} \int_0^\infty \frac{p^2\tau(p)D(p)\,{\rm d}p}{(\tau(k)+\tau(p))\,(\tau(\mu)+\tau(p))}. \quad (170)$$

It is precisely the condition that this expression should, indeed, yield a finite renormalized value which provides the required second relation, as we now explain.

In the inertial range limit, we seek scaling solutions with $\tau(k) \propto k^{-a}$ and $Q(k) \propto k^b$, in which case $D(k) = 2\tau(k)^{-1}Q(k) \propto k^{a+b}$. Now standard dimensional analysis shows that for (169) to hold in these circumstances, we must have $a+2b = -8$, [27]. Furthermore, if this scaling solution were to produce a non-renormalizable divergence in the response function, it would arise in the second term of (170), since we can assume that $a > 0$. To prevent this from occurring, the coefficient of the integral must be zero, which requires

$$\frac{\tau(k)}{\tau(\mu)} = \left(\frac{\mu}{k}\right)^{2/3}$$

giving $a = 2/3$, and, hence, $b = -11/3$, so that $a+b = -3$. Thus, these relations do, in fact, yield the solution (28) and (29), which we may conveniently re-write as

$$\tau(k)^{-1} = \beta\epsilon^{1/3}k^{2/3} \quad (171)$$

and

$$D(k) = \frac{\alpha}{2\pi}\epsilon^{2/3}k^{-3}. \quad (172)$$

Therefore, the energy spectrum function

$$E(k) = 4\pi k^2 Q(k) = 2\pi k^2 D(k)\tau(k)$$

takes the Kolmogorov inertial range form

$$E(k) = \alpha\epsilon^{2/3}k^{-5/3}$$

and the integral in the third term of (170) is, indeed, finite and yields

$$\Gamma(\boldsymbol{k}, 0) = \tau(k)^{-1}\left\{1 - g\log\left(\frac{k}{\mu}\right)\right\}.$$

For present purposes, explicit evaluation of the two constants is unnecessary, since they ultimately disappear from the calculation of the exponents, because they only occur through the coupling constant which, as we have seen, is eventually evaluated in terms of its fixed point value.

Next, we comment briefly on the effect of allowing for the perturbation terms (27) which give the difference between the modified quadratic form and the original viscous form. As in [10], we can treat these terms as being of nominal order g. Their effect is, firstly, to re-introduce into $\Gamma(\hat{k})$ the viscous timescale $\tau_\nu(k)$ which was replaced by $\tau_0(k)$. Secondly, and more significantly, new divergences appear. However, it is not difficult to show that the divergent terms which are independent of $h(k)$ and $\overline{\nu}$ sum exactly to the amount cancelled by the counterterms, as would be expected. In the inertial range limit $\overline{\nu} \to 0$, this leaves the term arising from $h(k)$, which is given by

$$\Delta\Gamma = -\frac{k^2}{\tau(k)}\int_0^\infty \frac{p^2 h(p)\,\mathrm{d}p}{\tau(k)^{-1} + \tau(p)^{-1}}.$$

Given that the actual stirring force spectrum function $h(k)$ has remained arbitrary, subject only to the condition that it yields a finite input power given by

$$4\pi\int_0^\infty p^2 h(p)\,\mathrm{d}p = \epsilon$$

it is clear that the above integral for $\Delta\Gamma$ must be finite.

Thus, the role of these perturbation terms is not critical as regards calculating the anomalous exponents, provided that the the spectrum of the stirring forces is non-zero only at small k, as it should be. However, what we find is that, although forced at large scales, the above solution behaves in the inertial range as if the fluid were stirred with a force spectral function $\propto k^{-3}$. In this context, it is interesting to note that, in a study of the randomly forced NS equations by a stochastic force with zero mean and variance $\propto k^{-3}$ [30], evidence of multiscaling of the structure functions has been found. In particular, the results obtained for the ratios ζ_n/ζ_2 with the k^{-3} spectrum have been shown to agree with the values computed from the NS equations forced at large scales. This, of course, is exactly what one might expect from the above approximation. The present results are also consistent with the numerical calculations in [31], which suggest the scaling $\tau_{\mathrm{L}}(k) \propto k^{-2/3}$, as in (171), for the Lagrangian micro-timescale, as opposed to the scaling $\tau_{\mathrm{E}}(k) \propto k^{-1}$ for the Eulerian micro-timescale, evidence for which has also been presented in [32]. As we have seen, the reason why the Lagrangian timescale applies in the present calculation is because we have eliminated sweeping by referring the velocity field to a frame moving with the local velocity of the large scale eddies which prevail at any chosen scale. This extracts the straining interactions, which shape the spectrum, from the background of convection, to yield quasi-Lagrangian approximations.

In a sense, this derivation of the Kolmogorov quadratic form is analogous to a multiple timescale expansion in nonlinear wave theory, where part of the nonlinear behaviour is

incorporated into the linear approximation, e.g. via a slowly changing wave amplitude, the variation of which is then determined from the nonlinear interaction by requiring the absence of secular terms in the higher order approximation. Here there is a similar solvability requirement which demands the absence of non-renormalizable terms, thereby determining the nonlinear behaviour of the modified quadratic form.

An integral part of the Kolmogorov theory is the exact result that in the inertial range limit

$$S_3(r) = -\tfrac{4}{5}\epsilon r \tag{173}$$

[5]. So we conclude this section by verifying that this result follows from the present treatment.

Using standard symmetry relations, we can express $S_3(r)$ in terms of the longitudinal component of the equal time triple velocity correlator

$$B_{\alpha\beta\gamma}(\boldsymbol{x}) = \left\langle v_\alpha(0)v_\beta(0)v_\gamma(\boldsymbol{x})\right\rangle$$

giving

$$S_3(r) = 6B_{111}(r, 0, 0). \tag{174}$$

Now the general form of the Fourier transform of $B_{\alpha\beta\gamma}$ must be

$$B_{\alpha\beta\gamma}(\boldsymbol{k}) = \mathrm{i}F(k)P_{\gamma\alpha\beta}(\boldsymbol{k})$$

and so $F(k)$ can be expressed in terms of the transfer spectrum $T(k)$ by

$$F(k) = \frac{\pi^2}{k^4}T(k)$$

while $T(k)$ is given to 1-loop order by (169). Substituting these results in (174) gives

$$S_3(r) = 12\mathrm{i}\pi \int \frac{T(k)}{k^4}k_1\left(1 - \frac{k_1^2}{k^2}\right)\exp(\mathrm{i}k_1 r)\,\mathrm{D}\boldsymbol{k}.$$

This integral can be expanded in powers of r the lowest-order term giving

$$S_3(r) = -12\pi^2 r \int \frac{T(k)}{k^4}k_1^2\left(1 - \frac{k_1^2}{k^2}\right)\mathrm{D}\boldsymbol{k}.$$

After integrating over the solid angle, we get

$$S_3(r) = -r\tfrac{4}{5}\int_\kappa^\infty T(k)\,\mathrm{d}k.$$

This latter integral is, of course, the transport power $\Pi_\mathrm{E}(\kappa)$, which is a finite quantity at 1-loop order and equal to the mean dissipation rate, as indicated in above, and, hence, we recover (173).

The correlation function $B_{111}(\boldsymbol{x})$ also has an important role in the derivation of the OPEs required for the structure functions with higher odd orders, as we shall see shortly.

9. Derivation of the OPEs

We give finally the derivation of the dominant terms of the OPEs which we have used in section 3 to obtain the structure function expansions relative to the moving frame. We deal first with the expansions required for the higher order structure functions with orders $n > 3$. These can be obtained using the technique described in [33]. We defer discussion of the particular case $n = 2$ until last, because it requires a different approach for the reasons given in section 3.

We begin by considering the OPE of the general product, defined in (55), as it appears in the expansion (56) for $S_n(r)$, taking first the case of even orders $n = 2m$, with $p = 0, 1, \ldots, m$, namely

$$\Lambda_{n-p,p}(\hat{x}, r) = \frac{v_+^{n-p} v_-^p}{p!(n-p)!}$$

where, as previously, $v_\pm = v_1(x \pm r/2, y, z, t)$, and we have used the definition (31), which applies in the moving frame. Let us consider the effect of inserting $\Lambda_{n-p,p}$ into a correlation function containing an arbitrary set of elementary fields $v_{\alpha_1}(\hat{x}), \ldots, v_{\alpha_l}(\hat{x}_l)$, as in (40). Then, following the approach of [33], we can derive the dominant terms which we have used in section 3 by considering how many of the v_+ fields can be paired with a v_- field to form products of lower-order correlation functions.

Consider the case $p = m$, i.e.

$$\langle v_{\alpha_1}(\hat{x}_1) \ldots v_{\alpha_l}(\hat{x}_l) \Lambda_{m,m}(\hat{x}, r) \rangle.$$

Here each v_+ can be paired with a v_- to yield a product term

$$\big\langle \big(v_+ v_-\big)^m \big\rangle \big\langle v_{\alpha_1}(\hat{x}_1) \ldots v_{\alpha_l}(\hat{x}_l) \big\rangle \tag{175}$$

which corresponds to the presence of a unit operator term in the OPE, [33]. If, instead, we only select $m-1$ pairs of $v_+ v_-$ products, we obtain a term of the type

$$2\big\langle \big(v_+ v_-\big)^{m-1} \big\rangle \left\langle v_{\alpha_1}(\hat{x}_1) \ldots v_{\alpha_l}(\hat{x}_l) \left(\frac{v_+^2}{2}\right) \right\rangle.$$

Now, in the limit as $r \to 0$, $v_+^2/2$ behaves like an insertion of $O_2(\hat{x})$ into the correlation function of elementary fields [33]. Hence, this product tends to

$$2\big\langle \big(v_+ v_-\big)^{m-1} \big\rangle \big\langle v_{\alpha_1}(\hat{x}_1) \ldots v_{\alpha_l}(\hat{x}_l) O_2(\hat{x}) \big\rangle. \tag{176}$$

But the averages of powers of $v_+ v_-$ simply yield non-stochastic functions of r, which we shall denote generically by $C_0(r), C_2(r), \ldots$, as appropriate. Thus, from (175) and (176), we obtain, in the limit as $r \to 0$,

$$\big\langle v_{\alpha_1}(\hat{x}_1) \ldots v_{\alpha_l}(\hat{x}_l) \Lambda_{m,m}(\hat{x}, r) \big\rangle = \big\langle v_{\alpha_1}(\hat{x}_1) \ldots v_{\alpha_l}(\hat{x}_l) \big[C_0(r) + C_2(r) O_2(\hat{x}) + \cdots \big] \big\rangle.$$

Since the elementary fields are arbitrary, it follows that we have an OPE of the form

$$\Lambda_{m,m}(\hat{x}, r) = C_0(r) I + C_2(r) O_2(\hat{x}) + \cdots.$$

The point about expansions of this type is that the operators of increasing complexity do, indeed, produce subdominant terms in the expansion of $S_n(r)$. Here, for example, the unit operator term, as we have shown, produces the dominant scaling with anomalous exponent given by (161), whereas the quadratic term can be readily shown to give the smaller exponent $\tau_n = [m(m-1) - 1]\Delta_2$, and, hence, is subdominant, while further terms in the expansion would produce even greater reductions.

A similar argument applies when $p = m - 1$. In this case, however, we cannot pair every v_+ with a v_-. Therefore, the unit operator term cannot appear in the OPE for $\Lambda_{m+1,m-1}$. If, however, we pair every v_- with a v_+ then the remaining v_+^2 pairs with the elementary fields and, in the limit as $r \to 0$, again appears as an $O_2(\hat{x})$ insertion. In this case, therefore, the OPE starts with $O_2(\hat{x})$ to give

$$\Lambda_{m+1,m-1}(\hat{x}, r) = C_2(r) O_2(\hat{x}) + \cdots.$$

By continuing with this argument, we see that the dominant term of the OPE for the general case of $\Lambda_{n-p,p}$ must take the form given in (57).

Consider next odd orders, $n = 2m + 1$. When $p = m$, we have a term of the form

$$\left\langle v_+^2 v_- \right\rangle \left\langle \left(v_+ v_-\right)^m \right\rangle \left\langle v_{\alpha_1}(\hat{x}_1) \dots v_{\alpha_l}\left(\hat{x}_l\right) \right\rangle$$

which, again, corresponds to the presence of a unit operator term, which is, thus, the dominant term of the OPE, giving

$$\Lambda_{m+1,m}(\hat{x}, r) = C_0(r) I + \cdots.$$

When $p = m - 1$, by pairing each v_- with a v_+, we obtain a term of the form

$$\left\langle \left(v_+ v_-\right)^{m-1} \right\rangle \left\langle v_{\alpha_1}\left(\hat{x}_1\right) \dots v_{\alpha_l}\left(\hat{x}_l\right) v_+^3 \right\rangle.$$

In the limit as $r \to 0$, v_+^3 appears as an insertion of the cubic operator $O_3(\hat{x})$, so that here the OPE takes the form

$$\Lambda_{m+2,m-1}(\hat{x}, r) = C_3(r) O_3(\hat{x}) + \cdots.$$

Continuing this process, we get for the next OPE

$$\Lambda_{m+3,m-2}(\hat{x}, r) = C_5(r) O_5(\hat{x}) + \cdots$$

and so on.

In fact, however, the only term which contributes to $S_n(r)$ for odd n is the unit operator term of $\Lambda_{m+1,m}$ because $\left\langle O_{2s+1}(\hat{x}) \right\rangle = 0$, for any integer s, in the case of homogeneous isotropic turbulence. The latter well known result follows from W by virtue of the fact that the relevant Feynman diagrams contain an odd number of NS vertices, one composite operator vertex and no external legs, so that any such diagram gives zero on integrating over the solid angles, because the NS vertex is an odd function of $\boldsymbol{k}$, whilst other factors are even. For example, in the case of $O_3(\hat{x})$, its lowest order term is given by the 2-loop diagram shown in figure 9, which contains one NS vertex and the O_3 vertex and has a symmetry factor of $1/2$. Hence, it yields a contribution to $\left\langle O_3(\hat{x}) \right\rangle$ given by

$$\left\langle O_3(\hat{x}) \right\rangle = \frac{\mathrm{i}}{2} \int P_{\alpha\beta\gamma}(\boldsymbol{l} + \boldsymbol{m}) P_{1\lambda}(\boldsymbol{l}) P_{1\mu}(\boldsymbol{m}) G_{\alpha\lambda}(\hat{l} + \hat{m}) Q_{\beta\mu}(\hat{l}) Q_{\gamma\nu}(\hat{m}) \, \mathrm{D}\hat{l} \, \mathrm{D}\hat{m}.$$

Substituting the zero-order correlator (78) and propagator (81), we get

$$\left\langle O_3(\hat{x}) \right\rangle = \frac{\mathrm{i}}{2} \int P_{1\beta\gamma}(\boldsymbol{l} + \boldsymbol{m}) P_{1\beta}(\boldsymbol{l}) P_{1\gamma}(\boldsymbol{m}) D(l) D(m) I(\boldsymbol{l}, \boldsymbol{m}) \, \mathrm{D}\boldsymbol{l} \, \mathrm{D}\boldsymbol{m} \qquad (177)$$

where

$$\begin{aligned} I(\boldsymbol{l}, \boldsymbol{m}) &= \frac{1}{(2\pi)^2} \int \frac{\mathrm{d}\Omega \, \mathrm{d}\Omega'}{[\Omega^2 + \sigma(l)^2][\Omega'^2 + \sigma(m)^2][\mathrm{i}(\Omega + \Omega') + \sigma(|\boldsymbol{l} + \boldsymbol{m}|)]} \\ &= \frac{1}{4\sigma(l)\sigma(m)[\sigma(l) + \sigma(m) + \sigma(|\boldsymbol{l} + \boldsymbol{m}|)]}. \end{aligned}$$

Clearly, the integrand in (177) changes sign under the transformation $(\boldsymbol{l}, \boldsymbol{m}) \to (-\boldsymbol{l}, -\boldsymbol{m})$, because all factors are even except for $P_{1\beta\gamma}(\boldsymbol{l} + \boldsymbol{m})$, which changes sign. It follows that the integral is zero.

In the particular case of $v_+ v_-$, we can establish the form of its OPE by using an expansion in the Fourier domain, in which the wavenumber q, corresponding to the separation r, tends to infinity, as described, for instance, in [7, 8]. To this end, we start by considering the general correlation function

$$H_{\alpha\beta\lambda\mu}(\hat{x}_1, \hat{x}_2 | \hat{x}', \hat{x}'') = \left\langle v_\alpha\left(\hat{x}_1\right) v_\beta\left(\hat{x}_2\right) v_\lambda\left(\hat{x}'\right) v_\mu\left(\hat{x}''\right) \right\rangle$$

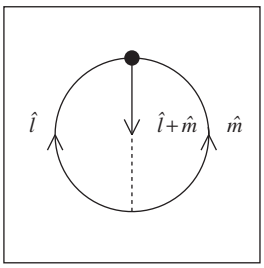

Figure 9. The 2-loop Feynman diagram for $\langle O_3(\hat{x})\rangle$.

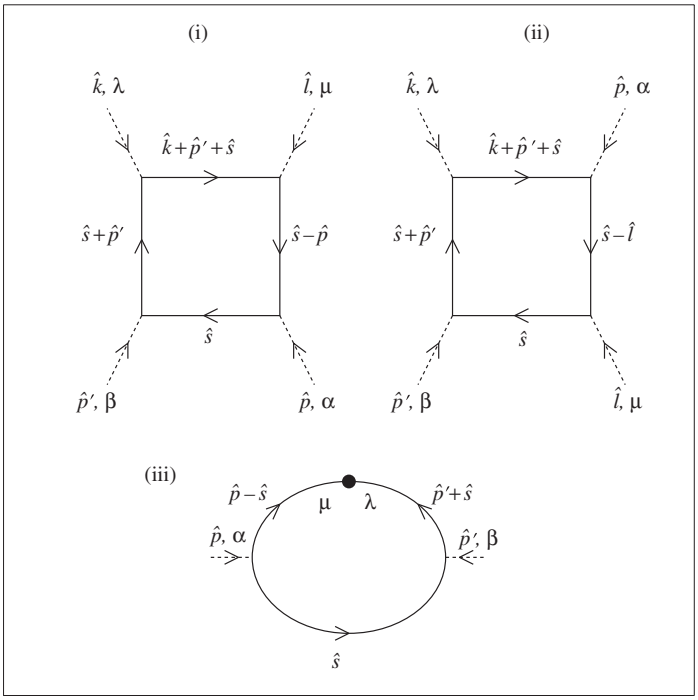

Figure 10. The 1-loop Feynman diagrams for the correlation functions evaluated in section 9 in connection with the OPEs.

for the case in which $\hat{x}'$ and $\hat{x}''$ tend to a common point $\hat{x}$, well separated from $\hat{x}_1$ and $\hat{x}_2$. For simplicity of presentation here, we have included only two arbitrary fields $v_\alpha(\hat{x}_1)$ and $v_\beta(\hat{x}_2)$. Denote its Fourier transform by

$$\begin{aligned} H_{\alpha\beta\lambda\mu}(\hat{p},\,\hat{p}'|\hat{k},\,\hat{k}') &= \left\langle v_\alpha\big(\hat{p}\big)v_\beta\big(\hat{p}'\big)v_\lambda(\hat{k})v_\mu(\hat{k}')\right\rangle \\ &= (2\pi)^4\,\delta(\hat{p}+\hat{p}'+\hat{k}+\hat{k}')\tilde{H}_{\alpha\beta\lambda\mu}(\hat{p},\,\hat{p}'|\hat{k},\,\hat{k}'). \end{aligned} \tag{178}$$

Then, in terms of the reduced correlation function, we can write

$$\begin{aligned} H_{\alpha\beta\lambda\mu}(\hat{x}_1,\hat{x}_2|\hat{x}',\hat{x}'') = \int \mathrm{D}\hat{p}\,\mathrm{D}\hat{p}'\,\mathrm{D}\hat{q}\;\tilde{H}_{\alpha\beta\lambda\mu}\left(\hat{p},\,\hat{p}'\,\middle|\,\hat{q}-\frac{\hat{p}+\hat{p}'}{2},-\hat{q}-\frac{\hat{p}+\hat{p}'}{2}\right) \\ \times\exp\left\{\mathrm{i}\hat{p}\cdot\left(\hat{x}_1-\frac{\hat{x}'+\hat{x}''}{2}\right)+\mathrm{i}\hat{p}'\cdot\left(\hat{x}_2-\frac{\hat{x}'+\hat{x}''}{2}\right)+\mathrm{i}\hat{q}\cdot\big(\hat{x}'-\hat{x}''\big)\right\}. \end{aligned} \tag{179}$$

When the arguments in (178) coalesce to the common point $\hat{x}$, we obtain the correlation function

$$Q_{\alpha\beta\lambda\mu}(\hat{x}_1, \hat{x}_2|\hat{x}) = \left\langle v_\alpha\left(\hat{x}_1\right) v_\beta\left(\hat{x}_2\right) v_\lambda\left(\hat{x}\right) v_\mu\left(\hat{x}\right)\right\rangle$$

with Fourier transform

$$\begin{aligned} Q_{\alpha\beta\lambda\mu}(\hat{p}, \hat{p}'|\hat{q}) &= \left\langle v_\alpha\left(\hat{p}\right) v_\beta\left(\hat{p}'\right)\left(v_\lambda v_\mu\right)\left(\hat{q}\right)\right\rangle \\ &= (2\pi)^4\,\delta(\hat{p}+\hat{p}'+\hat{q})\tilde{Q}_{\alpha\beta\lambda\mu}(\hat{p}, \hat{p}'|\hat{q}). \end{aligned}$$

Thus, corresponding to (179), we have

$$Q_{\alpha\beta\lambda\mu}(\hat{x}_1, \hat{x}_2|\hat{x}) = \int \mathrm{D}\hat{p}\,\mathrm{D}\hat{p}'\, Q_{\alpha\beta\lambda\mu}(\hat{p}, \hat{p}'|-\hat{p}-\hat{p}')\exp\left\{\mathrm{i}\hat{p}\cdot\left(\hat{x}_1-\hat{x}\right)+\mathrm{i}\hat{p}\cdot\left(\hat{x}_2-\hat{x}\right)\right\}.$$

Let $\Psi_{\alpha\beta\lambda\mu}(\hat{p}, \hat{p}'|\hat{k}, \hat{k}')$ and $\Xi_{\alpha\beta\lambda\mu}(\hat{p}, \hat{p}'|\hat{q})$ be the 1PI functions associated with the connected parts of $\tilde{H}_{\alpha\beta\lambda\mu}(\hat{p}, \hat{p}'|\hat{k}, \hat{k}')$ and $\tilde{Q}(\hat{p}, \hat{p}'|\hat{q})$. We consider the specific vertex shown in figure 10, the treatment of the other three vertex functions associated with (178) being similar. Denoting the connected part by superscript c, we have, as in section 5,

$$\tilde{H}^{(c)}_{\alpha\beta\lambda\mu}(\hat{p}, \hat{p}'|\hat{k}, \hat{k}') = -G_{\alpha\alpha'}\left(\hat{p}\right) G_{\beta\beta'}\left(\hat{p}'\right) G_{\lambda\lambda'}(\hat{k}) G_{\mu\mu'}(\hat{k}')\Psi_{\alpha'\beta'\lambda'\mu'}(\hat{p}, \hat{p}'|\hat{k}, \hat{k}') \tag{180}$$

and

$$\tilde{Q}^{(c)}_{\alpha\beta\lambda\mu}(\hat{p}, \hat{p}'|\hat{q}) = -G_{\alpha\alpha'}(\hat{p}) G_{\beta\beta'}(\hat{p}')\Xi_{\alpha'\beta'\lambda\mu}(\hat{p}, \hat{p}'|\hat{q}). \tag{181}$$

According to the standard procedure [7, 8], the behaviour of the correlation function $H_{\alpha\beta\lambda\mu}(\hat{x}_1, \hat{x}_2|\hat{x}', \hat{x}'')$ as a function of $\hat{x}'-\hat{x}''$, when $\hat{x}'$ and $\hat{x}''$ both tend to a common value $\hat{x}$, can be deduced from the behaviour of $\Psi_{\alpha\beta\lambda\mu}(\hat{p}, \hat{p}'|\hat{q}-(\hat{p}+\hat{p}')/2, -\hat{q}-(\hat{p}+\hat{p}')/2)$, in the limit as $\hat{q}\to\infty$, which is, indeed, apparent from (179) and (180). Now, the diagrams which contribute to this 1PI correlation function are diagram (i) of figure 9, together with its permutation $(\hat{p}, \alpha)\leftrightarrow(\hat{p}', \beta)$, and diagram (ii). However, it is easy to see from these diagrams that, as $\hat{q}\to\infty$, diagram (ii) yields a contribution which is smaller than that from diagram (i) by a factor $Q_{\sigma\nu}(\hat{q})\sim q^{-11/3}$. So to derive the dominant term, we need to focus on diagram (i) and its permutation. The corresponding diagrams for $\Xi_{\alpha\beta\lambda\mu}(\hat{p}, \hat{p}'|-\hat{p}-\hat{p}')$ are diagram (iii) of figure 9 plus its permutation $\lambda\leftrightarrow\mu$.

Evaluation of these diagrams using the Feynman rules is straightforward and yields

$$\begin{aligned} &\Psi_{\alpha\beta\lambda\mu}\left(\hat{p}, \hat{p}'\left|\hat{q}-\frac{\hat{p}+\hat{p}'}{2}, -\hat{q}-\frac{\hat{p}+\hat{p}'}{2}\right.\right) \\ &\quad= \int P_{\lambda\xi\rho}\left(\boldsymbol{q}-\frac{\boldsymbol{p}+\boldsymbol{p}'}{2}\right) P_{\mu\tau\eta}\left(-\boldsymbol{q}-\frac{\boldsymbol{p}+\boldsymbol{p}'}{2}\right) P_{\alpha\gamma\sigma}(\boldsymbol{p}) P_{\beta\nu\delta}(\boldsymbol{p}') \\ &\qquad\times Q_{\gamma\delta}(\hat{s}) Q_{\eta\sigma}(\hat{p}-\hat{s}) Q_{\xi\nu}(\hat{p}'+\hat{s}) Q_{\rho\tau}\left(\hat{q}+\frac{\hat{p}'-\hat{p}}{2}+\hat{s}\right)\mathrm{D}\hat{s} + (\hat{p}, \alpha) + (\hat{p}', \beta) \end{aligned}$$

and

$$\begin{aligned} \Xi_{\alpha\beta\lambda\mu}(\hat{p}, \hat{p}'|-\hat{p}-\hat{p}') &= -\int P_{\alpha\sigma\gamma}(\boldsymbol{p}) P_{\beta\nu\delta}(\boldsymbol{p}') Q_{\gamma\delta}(\hat{s}) Q_{\sigma\mu}(\hat{p}-\hat{s}) Q_{\lambda\nu}(\hat{p}'+\hat{s})\,\mathrm{D}\hat{s} \\ &\quad+(\lambda\leftrightarrow\mu). \end{aligned}$$

Hence, for large $\hat{q}$, we obtain from the last two equations the relation

$$\begin{aligned} &\Psi_{\alpha\beta\lambda\mu}\left(\hat{p}, \hat{p}'\left|\hat{q}-\frac{\hat{p}+\hat{p}'}{2}, -\hat{q}-\frac{\hat{p}+\hat{p}'}{2}\right.\right) \\ &\quad= P_{\lambda\xi\rho}(\boldsymbol{q}) P_{\mu\tau\eta}(\boldsymbol{q}) Q_{\rho\tau}(\hat{q})\Xi_{\alpha\beta\xi\eta}(\hat{p}, \hat{p}'|-\hat{p}-\hat{p}'). \end{aligned}$$

Combining this with (180) and (181) yields the approximation

$$H^{(c)}_{\alpha\beta\lambda\mu}\left(\hat{p},\,\hat{p}'\,\middle|\,\hat{q}-\frac{\hat{p}+\hat{p}'}{2},\,-\hat{q}-\frac{\hat{p}+\hat{p}'}{2}\right)=C_{\lambda\mu\xi\eta}(\hat{q})\,Q^{(c)}_{\lambda\mu\xi\eta}(\hat{p},\,\hat{p}'|-\hat{p}-\hat{p}') \tag{182}$$

where, to this order,

$$C_{\lambda\mu\xi\eta}(\hat{q})=P_{\lambda\xi\rho}(\boldsymbol{q})P_{\mu\tau\eta}(\boldsymbol{q})\left|G(\hat{q})\right|^2 Q_{\rho\tau}(\boldsymbol{q}). \tag{183}$$

To obtain the required expansion for v_+v_-, we must take the inverse Fourier transform of (182) for the particular case $\lambda=\mu=1$ with

$$\hat{x}'=\left(x+\frac{r}{2},\,y,\,z,\,t\right)\qquad\text{and}\qquad\hat{x}''=\left(x-\frac{r}{2},\,y,\,z,\,t\right).$$

The coefficient $C_{11\xi\eta}(\hat{x}'-\hat{x}'')$ then depends only upon r and, according to (183), it must have the form

$$C_{11\xi\eta}(r)=\int\frac{q_\xi q_\eta(q_2^2+q_3^2)}{q^4}F(q)\exp(-\mathrm{i}q_1r)\,\mathrm{D}\boldsymbol{q}$$

where $F(q)$ is a function only of the wavenumber q. It is clear from this integral that $C_{11\xi\eta}$ must be diagonal in the indices ξ, η, and have equal transverse components: $C_{1122}=C_{1133}$.

We now define $Q^{(L)}_{\alpha\beta}(\hat{x}_1,\hat{x}_2|\hat{x})$ to be the connected correlation function formed from the elementary fields $v_\alpha(\hat{x}_1)$ and $v_\beta(\hat{x}_2)$, with the insertion of the longitudinal energy operator $O_2(\hat{x})$, ie it is the particular case of (42) with $s=2$ and $l=2$. Then

$$Q^{(c)}_{\alpha\beta11}(\hat{x}_1,\hat{x}_2|\hat{x})=2Q^{(L)}_{\alpha\beta}(\hat{x}_1,\hat{x}_2|\hat{x}).$$

Similarly, we define $Q^{(T)}_{\alpha\beta}(\hat{x}_1,\hat{x}_2|\hat{x})$ to be the correlation function with $v_\alpha(\hat{x}_1)$ and $v_\beta(\hat{x}_2)$, and the insertion of the transverse energy operator

$$O^{(T)}_2(\hat{x})=\tfrac{1}{2}\big(v_2^2+v_3^2\big).$$

Thus, we have

$$Q^{(c)}_{\alpha\beta22}(\hat{x}_1,\hat{x}_2|\hat{x})+Q^{(c)}_{\alpha\beta33}(\hat{x}_1,\hat{x}_2|\hat{x})=2Q^{(T)}_{\alpha\beta}(\hat{x}_1,\hat{x}_2|\hat{x}).$$

Finally, we define longitudinal and transverse coefficients by writing

$$C_2(r)=2C_{1111}(r)$$

and

$$C_2(r)=2C_{1122}(r)=2C_{1133}(r).$$

Using these definitions, and taking into account the diagonality of $C_{11\xi\eta}$, enables us to express the inverse Fourier transform of (182), for the case $\lambda=\mu=1$, as

$$H^{(c)}_{\alpha\beta11}(\hat{x}_1,\hat{x}_2|\hat{x},r)=C_2(r)Q^{(L)}_{\alpha\beta}(\hat{x}_1,\hat{x}_2|\hat{x})+C_2'(r)Q^{(T)}_{\alpha\beta}(\hat{x}_1,\hat{x}_2|\hat{x})$$

which, in the limit as $r\to0$, leads to

$$\langle v_\alpha(\hat{x}_1)v_\beta(\hat{x}_2)v_+v_-\rangle=\left\langle v_\alpha(\hat{x}_1)v_\beta(\hat{x}_2)\left[\frac{E}{3}+C_2(r)O_2(\hat{x})+C_2(r)O^{(T)}_2(\hat{x})+\cdots\right]\right\rangle.$$

Since the fields $v_\alpha(\hat{x}_1)$ and $v_\beta(\hat{x}_2)$ are arbitrary, we may conclude that

$$v_+v_-=\frac{E}{3}I+C_2(r)O_2(\hat{x})+\cdots.$$

Note that we have discarded the transverse operator because it is subdominant. This follows immediately from the analysis of section 5. For example, in the case of $O^{(T)}_2$, when we calculate the corresponding value of the constant $a^{(2)}_1$, as defined in (135), we get twice the

value given in (150) for the longitudinal operator $O_2(\hat{x})$, because, by isotropy, each of the two transverse components of $O_2^{(T)}(\hat{x})$ contributes an amount equal to the value obtained for $O_2(\hat{x})$ and, hence, the right hand side of (159) then yields an anomalous exponent of $2\Delta_2$, indicating that $O_2^{(T)}(\hat{x})$ makes a subdominant contribution to $S_2(r)$. Thus, we have shown, to within the order g^2 of the calculation, that the dominant term of the OPE for v_+v_- has the form given in (39).

10. Summary and discussion

The fact that it has been possible to demonstrate multiscaling and calculate anomalous exponents successfully from the generating functional by means of perturbation theory, notwithstanding the strong nonlinearity of the NS equations, is attributable to several factors. These include: (1) the use of a modified quadratic form, which is derived self-consistently from the NS nonlinearity; (2) the incorporation in the generating functional of the composite operators which appear in the definition of the general structure function; (3) the application of OPEs to derive corrections to the Kolmogorov exponents in terms of the anomalous dimensions of these operators; (4) the identification of a class of irreducible Green functions containing insertions of these operators, which facilitate the calculation of their anomalous dimensions; (5) the elimination of sweeping convection effects using a random Galilean transformation of the velocity field; and, finally, (6) the deduction of the inertial range scaling using an uv fixed point of the RG to achieve the required small wavenumber limit. Let us now consider how each of these factors contributes to overcoming the obstacles encountered in previous applications of the RG.

The use of the modified quadratic form is an important element in the success of our calculation, because it provides an accurate initial approximation, which yields the Kolmogorov distribution in the inertial range limit. By contrast, in the early work which employed a field theoretic RG [34], and in subsequent developments of it [35–37], including equivalent formulations based on [38], reviewed recently in [39], the zero-order approximation is based solely on on the linear terms of the NS equations, as in a conventional field theory calculation. Because this is a poor approximation for turbulence, it does not result in a genuine weak expansion parameter. For example, in the previous applications of RG techniques based on an expansion in the force spectrum exponent (i.e. the ϵ-expansion), in which the expansion about $\epsilon = 0$ is extrapolated to $\epsilon = 4$, the value of the coupling constant is not small, at the ir fixed point which is used. Therefore, the accuracy of the expansion is uncontrolled. Indeed, according to [40], it may even be uncontrolled when $\epsilon \ll 1$, and there are problems in establishing its radius of convergence and the value of ϵ at which long range driving becomes technically irrelevant [41].

However, our expansion is of a different nature. First, we do not use an ϵ-expansion. Actually, there is no force power spectrum in our calculation as such. As we showed, the force spectrum $h(k)$ remains in the calculation as an arbitrary function, subject only to the requirment that it yields a finite input power. What the modified quadratic form provides, however, is an apparent force power spectrum $D(k)$, but its exponent is fixed by the solution (172), and, thus, cannot be varied. Second, we do not use an ir fixed point, because we are interested in taking the short wavelength limit, for which purpose we require an uv fixed point. Together, these differences result in a genuinely small coupling constant g, which is about $1/20$ at the fixed point, as shown in section 4. Hence, our expansion is inherently more accurate than the ϵ-expansion. In fact, given that our calculation is carried out to 2-loop order, its errors are controlled at $g^3 \sim 10^{-4}$. Another significant consequence of using the modified quadratic form is that no convergence problems are encountered in the uv region. This, together with the

fact that we do not use an ϵ-expansion or an ir fixed point, means that none of the ingredients which cause marginality by power counting in previous applications of the RG [40], are present in our approach.

On the other hand, there is a similar problem to be faced in the present calculation. Any fully renormalized theory of turbulence must contain an infinite number of renormalized functions because it must be equivalent to the hierarchy of equations for the cumulants. This equivalence has been demonstrated recently [42]. In fact, each cumulant will have a representation as a expansion in terms of irreducible renormalized functions. Thus, one has an infinite set of vertex functions to contend with. Now, when any one of these irreducible functions is calculated in perturbation theory using the modified quadratic form, the overall logarithmic divergence will remain, after sweeping divergences have been eliminated. So the problem in the present approach amounts to the resummation of these logarithms. However, we showed in section 5 that this difficulty could be overcome, in relation to multiscaling, by identifying the infinite sub-class of functions which yields the desired information relating to anomalous exponents while being, at the same time, amenable to resummation using the RG. The irreducible inserted nonlinear Green functions defined in section 5 satisfy both requirements. Being fully irreducible they give full n-point correlations. However, as we have seen, to render them tractable, it was expedient to obtain a mean response to forcing at the centroid of the excitation points. This averaging thus constitutes a closure approximation. Although this type of closure approximation permits considerable progress to be made with the calculation of the exponents, the averaging process limits its applicability to relatively low orders, $n \lesssim 10$, because the multiple correlations between the apparent forcing at different space–time points are not then approximated accurately enough at higher orders. Thus, a different approximation would be required to obtain the asymptotic scaling at large orders and it remains for future work to discover a suitable approach.

References

[1] Nelkin M 1994 Universality and scaling in fully developed turbulence *Adv. Phys.* **43** 143
[2] Sreenivasan K R and Antonia R A 1997 The phenomenology of small scale turbulence *Annu. Rev. Fluid Mech.* **29** 435
[3] Sreenivasan K R Fluid turbulence 1999 *Rev. Mod. Phys.* **71** S383
[4] Kolmogorov A N 1941 Local structure of turbulence in an incompressible fluid for very large Reynolds numbers *Dokl. Acad. Nauk. SSSR* **30** 299
[5] Frisch U 1995 *Turbulence* (Cambridge: Cambridge University Press)
[6] McComb W D 1996 *The Physics of Fluid Turbulence* (Oxford: Clarendon)
[7] Zinn-Justin J 1996 *Quantum Field Theory* (Oxford: Clarendon)
[8] Collins J C 1984 *Renormalisation* (Cambridge: Cambridge University Press)
[9] Martin P C, Siggia E D and Rose H A 1973 Statistical dynamics of classical systems *Phys. Rev.* A **8** 423
[10] Edwards S F and McComb W D 1969 Statistical mechanics far from equilibrium *J. Phys. A: Math. Gen.* **2** 157
[11] Bazdenkov S V and Kukharkin N N 1993 On the variational method of closure in the theory of turbulence *Phys. Fluids* A **5** 2248
[12] Pokorski S 1987 *Gauge Field Theories* (Cambridge: Cambridge University Press)
[13] Le Bellac M 1991 *Quantum and Statistical Field Theory* (Oxford: Clarendon)
[14] Teodorovich E V 1994 Diagram equations of the theory of fully developed turbulence *Theor. Math. Phys.* **101** 1177
[15] L'vov V and Procaccia I 1995 Exact resummations in the theory of hydrodynamic turbulence I. The ball of locality and normal scaling *Phys. Rev.* E **52** 3840
[16] L'vov V and Procaccia I 1995 Exact resummations in the theory of hydrodynamic turbulence II. A ladder to anomalous scaling *Phys. Rev.* E **52** 3858
[17] Binney J J, Dowrick N J, Fisher A J and Newman M E J 1992 *The Theory of Critical Phenomena* (Oxford: Clarendon)
[18] Teodorovich E V 1989 A hydrodynamic generalisation of Ward's identity *Prikl. Mat. Mekhan.* **53** 340

[19] Benzi R, Ciliberto S, Tripiccione R, Baudet C, Massaioli F and Succi S 1993 Extended self-similarity in turbulent flows *Phys. Rev.* E **48** R29
[20] van de Water W, van der Vorst B and van de Wetering E 1991 Multiscaling of turbulent structure functions *Europhys. Lett.* **16** 443
[21] Anselmet F, Gagne Y, Hopfinger E J and Antonia R A 1984 High-order velocity structure functions in turbulent sheer flows *J. Fluid Mech.* **140** 63
[22] Belin F, Tabeling P and Willaime H 1996 Exponents of the structure functions in a low temperature helium experiment *Physica* D **93** 52
[23] Sreenivasan K R and Dhruva B 1998 Is there scaling in high Reynolds number turbulence? *Prog. Theor. Phys.* (Suppl.) **130** 103
[24] Kraichnan R H 1959 The structure of isotropic turbulence at very high Reynolds numbers *J. Fluid Mech.* **5** 497
[25] Kadomtsev B B 1995 *Plasma Turbulence* (Reading, MA: Academic)
[26] Kraichnan R H 1965 Lagrangian history closure approximation for turbulence *Phys. Fluids* **8** 575
[27] Leslie D C 1973 *Developments in the Theory of Turbulence* (Oxford: Clarendon)
[28] Yakhot V 1981 Ultraviolet dynamic renormalisation group *Phys. Rev.* A **23** 1486
[29] L'vov V S 1991 Scale invariant theory of fully developed turbulence-Hamiltonian approach *Phys. Rep.* C **207** 1
[30] Sain A, Manu and Pandit R 1998 Turbulence and multiscaling in the randomly forced Navier–Stokes equation *Phys. Rev. Lett.* **81** 4377
[31] Kaneda Y, Ishihara T and Gotoh K 1999 Taylor expansions in powers of time of Lagrangian and Eulerian two-point two-time velocity correlations in turbulence *Phys. Fluids* **11** 2154
[32] Hayot F and Jayaprakash C 1998 Dynamic structure factors in models of turbulence *Phys. Rev.* E **57** R4867
[33] Cardy J 1997 *Scaling and Renormalisation in Statistical Physics* (Cambridge: Cambridge University Press)
[34] DeDominicis C and Martin P C 1979 Energy spectra of certain randomly-stirred fluids *Phys. Rev.* A **19** 419
[35] Bhattacharjee J K 1988 Randomly stirred fluids, mode coupling theories and the turbulent Prandtl number *J. Phys. A: Math. Gen.* **21** L551
[36] Teodorovich E V 1989 On the calculation of the Kolmogorov constant in a description of turbulence by means of the renormalisation group method *Sov. Phys.–JETP* **69** 89
[37] Ronis D 1987 Field theoretic renormalisation group and turbulence *Phys. Rev.* A **36** 3322
[38] Yakhot V and Orszag S A 1986 Renormalisation group analysis of turbulence *Phys. Rev. Lett.* **57** 1722
[39] Smith L M and Woodruff S L 1998 Renormalisation group analysis of turbulence *Ann. Rev. Fluid Mech.* **30** 275
[40] Eyink G L 1994 The renormalisation group method in statistical hydrodynamics *Phys. Fluids* **6** 3063
[41] Mou C Y and Weichman P B 1995 Multicomponent turbulence, the spherical limit, and non-Kolmogorov spectra *Phys. Rev.* E **52** 3738
[42] L'vov V S and Procaccia I 1998 Computing the scaling exponents in fluid turbulence from first principles: the formal setup *Physica* A **257** 165